THE JOURNAL OF PHYSICAL CHEMISTRY A

Article

pubs.acs.org/JPCA

Computational Study of the Hydration of Sulfuric Acid Dimers: Implications for Acid Dissociation and Aerosol Formation

Berhane Temelso, Thuong Ngoc Phan, and George C. Shields*

Dean's Office, College of Arts and Sciences, and Department of Chemistry, Bucknell University, Lewisburg, Pennsylvania 17837, United States

Supporting Information

ABSTRACT: We have investigated the thermodynamics of sulfuric acid dimer hydration using ab initio quantum mechanical methods. For $(H_2SO_4)_2(H_2O)_n$ where n = 0−6, we employed high-level ab initio calculations to locate the most stable minima for each cluster size. The results presented herein yield a detailed understanding of the first deprotonation of sulfuric acid as a function of temperature for a system consisting of two sulfuric acid molecules and up to six waters. At 0 K, a cluster of two sulfuric acid molecules and one water remains undissociated. Addition of a second water begins the deprotonation of the first sulfuric acid leading to the di-ionic species (the bisulfate anion HSO_4^-, the hydronium cation H_3O^+, an undissociated sulfuric acid molecule, and a water). Upon the addition of a third water molecule, the second sulfuric acid molecule begins to dissociate. For the $(H_2SO_4)_2(H_2O)_3$ cluster, the di-ionic cluster is a few kcal mol^{-1} more stable than the neutral cluster, which is just slightly more stable than the tetra-ionic cluster (two bisulfate anions, two hydronium cations, and one water). With four water molecules, the tetra-ionic cluster, $(HSO_4^-)_2(H_3O^+)_2(H_2O)_2$, becomes as favorable as the di-ionic cluster $H_2SO_4(HSO_4^-)(H_3O^+)(H_2O)_3$ at 0 K. Increasing the temperature favors the undissociated clusters, and at room temperature we predict that the di-ionic species is slightly more favorable than the neutral cluster once three waters have been added to the cluster. The tetra-ionic species competes with the di-ionic species once five waters have been added to the cluster. The thermodynamics of stepwise hydration of sulfuric acid dimer is similar to that of the monomer; it is favorable up to n = 4−5 at 298 K. A much more thermodynamically favorable pathway forming sulfuric acid dimer hydrates is through the combination of sulfuric acid monomer hydrates, but the low concentration of sulfuric acid relative to water vapor at ambient conditions limits that process.

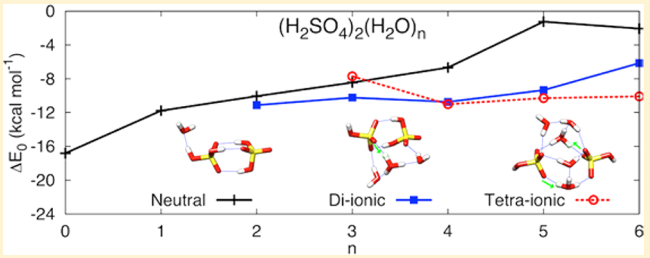

1. INTRODUCTION

Hydration of acids plays a key role in the atmosphere[1] as a source of aerosol nucleation intermediates and catalytic agents in many reactions. As such, an accurate physical understanding of these phenomena is essential for modeling atmospheric processes.[2] Atmospheric aerosols are thought to have a significant cooling effect on the global climate, but the extent of the effect is uncertain.[3] The forcing effects of aerosols remain the most uncertain parameters in atmospheric studies of global warming,[3−6] which makes the study of aerosol formation one of the most important endeavors today. The direct scattering of incoming radiation causes atmospheric cooling, whereas absorption can cause atmospheric warming. The increasing extent of water itself in the lower atmosphere has significant implications for global warming.[1,7,8] A small number of nanoscale aerosols grow to much larger cloud condensation nuclei (CCN) and change the precipitation efficiency of clouds as well as cause a cooling effect because of increased cloud albedo.

Aerosols are particulate matter suspended in a gas. Primary aerosols are directly injected into the atmosphere whereas secondary aerosols form in the atmosphere through physical and chemical interactions of condensable vapors. The main molecular player in secondary aerosol formation is sulfuric acid because it is easily formed in the atmosphere from the oxidation of SO_2 and serves as an effective nucleating species.[6] Experimental observations over a very broad range of atmospheric and laboratory conditions have shown that new particle formation depends on the concentration of sulfuric acid.[9−13] The formation of new particles proceeds through two phases: a nucleation phase leading to a metastable critical cluster (∼1−3 nm in diameter) and a growth phase where the critical cluster increases readily in size.[14,15] Besides binary homogeneous nucleation (BHN) of sulfuric acid and water, ternary nucleation (THN) involving ammonia and amines and those incorporating organic acids[16−19] and ions (IIN)[20−22] are expected to be significant in the continental boundary layer.[23] Even though small particles less than 3 nm in diameter initiate aerosol formation,[10] our insight into this process is incomplete because the size detection of experimental apparati has been

Received: June 3, 2012
Revised: August 12, 2012
Published: September 4, 2012

dx.doi.org/10.1021/jp3054394 | J. Phys. Chem. A 2012, 116, 9745−9758

limited to 3 nm or larger in diameter until recent advances extended it to 1.3−1.5 nm.[10,24−26] The challenge of detecting, counting, and determining the exact composition of these molecular clusters as they grow to a critical cluster has hindered the development of models of aerosol activation and growth based solely on experiment.[27−29]

Most theoretical studies of sulfuric acid/water nucleation use a version of classical nucleation theory (CNT) that models new particle formation based on bulk properties such as surface tension, molar volume, partial molar volumes, vapor pressures, and equilibrium vapor pressures.[30−43] Current models of secondary aerosol formation largely underestimate what is observed in the atmosphere.[9,13,24,44−47] One of the reasons for this discrepancy could be the hydration of sulfuric acid. Sulfuric acid forms hydrates even at low (<20%) relative humidity,[48,49] decreasing the number of free acid monomers, stabilizing the vapor and increasing the nucleation barrier such that CNT nucleation rates are reduced by a factor of 10^3−10^8 compared to those in the absence of hydration.[41,49] To incorporate the effect of hydration on nucleation rates, many models have used a combination of experimental[50] and theoretical equilibrium constants of hydration.[41,47] Experimental equilibrium constants' error bars[50] are large and computed values vary substantially for density functional theory (DFT)[51−56] and ab initio methods.[57,58] The most reliable computational studies of sulfuric acid hydrate formation to date are from the Helsinki group,[58] who have shown that MP2 ab initio calculations extrapolated to the complete basis set limit and corrected for vibrational anharmonicity yield equilibrium constants of hydration that are close to the available experimental values of Hanson and Eisele,[50] and from our group.[59] Our recent paper introduced an improved basis set extrapolation scheme, accounted for molecular symmetry for finite temperature corrections, extended the study of H_2SO_4 to hexahydrates, explored a larger configurational space for the hydrate isomers, incorporated all low-lying isomers into the final energies by Boltzmann averaging, and updated the discussion with the most recent experimental results on the sulfuric acid−water system. In this paper we extend our previous work on a single sulfuric acid to two sulfuric acids with up to six water molecules. We searched for the minimum energy structures of sulfuric acid hydrates $(H_2SO_4)_2(H_2O)_{n=0-6}$ and determined the thermodynamic properties of these clusters. The computed Gibbs free energies were used to estimate the concentrations of the hydrates at three temperatures germane to the troposphere. We used these results to gain further insight into the binary nucleation of sulfuric acid and water, as well as the nature of acid dissociation at a molecular level. This work is a continuation of long-standing efforts to explore ion−molecule interactions,[60−69] hydrogen-bonded interactions,[70−82] water cluster formation,[65,70,71,81,83−91] and atmospheric processes.[59,66−69,92−97]

2. METHODOLOGY

An initial set of configurations for $(H_2SO_4)_2(H_2O)_{n=0-6}$ were taken from Ding et al.'s[98] DFT study. Removing waters from large clusters and using them as starting structures for smaller clusters generated a larger number of configurations. We have previously applied a two-step gas-phase molecular dynamics (MD) sampling scheme to studies of $CS_2(H_2O)_{n=1-4}$, $OCS(H_2O)_{n=1-4}$, $NH_4^+(H_2O)_{n=5-10}$, $H_2SO_4(H_2O)_{n=4-6}$, $HSO_4^-(H_2O)_{n=3-6}$, and $(H_2O)_{n=7,9,10}$ clusters,[59,68,69,88−91,94,97] but such an approach was not necessary here because Ding et al.'s[98] have performed a thorough search of the low energy structures for this system. With the exception of a few reactive model potentials that allow proton transfer, classical force fields cannot yield dissociated clusters starting with neutral ones. Ding et al.'s potential[54] has explicit parameters for H_2SO_4, HSO_4^-, H_3O^+, and H_2O, thereby providing structures of varying acid dissociation. However, quantum mechanical optimizations can locate minima of type I, II, and III starting with undissociated (I) structures. The structures were optimized at the second-order Møller−Plesset perturbation theory (MP2) level with the 6-31+G* basis set enforcing strict convergence criteria (rms gradient $<1 \times 10^{-5}$ au/Å and rms displacement $<4 \times 10^{-5}$ Å) using Gaussian 09.[99] The converged minima were subject to single-point energy calculations with the resolution of the identity MP2 (RI-MP2) method[100,101] using ORCA 2.8.0.[102] We obtained RI-MP2 complete basis set (CBS) binding energies using Dunning's augmented correlation-consistent basis sets (aug-cc-pVNZ, N = D, T, Q)[103−105] and corresponding auxiliary basis sets.[106] In the results that follow we denote Dunning's aug-cc-pVNZ basis sets by aVNZ.

To obtain accurate interaction energies of these non-covalently bonded systems, we followed past practice and extrapolated the energy to the CBS limit. The RI-MP2/CBS limit was estimated using the 4−5 inverse polynomial extrapolation[107,108] that has been used extensively for water clusters:

$$E_N^{\text{RI-MP2}} = E_{\text{CBS}}^{\text{RI-MP2}} + \frac{b}{(N+1)^4} + \frac{c}{(N+1)^5} \quad (1)$$

where $E_N^{\text{RI-MP2}}$ is the RI-MP2/aVNZ//MP2/6-31+G* energy, $E_{\text{CBS}}^{\text{RI-MP2}}$ is the extrapolated RI-MP2/CBS//6-31+G* energy, N is the largest angular momentum number for the aVNZ basis set (N = 2, 3, 4 for N = D, T, Q, respectively), and b and c are fitting parameters.[107,109] We have demonstrated that the 4−5 inverse polynomial extrapolation (eq 1) scheme performs better than Halkier's conventional basis set extrapolation for water clusters, sulfuric acid hydrates and bisulfate hydrates.[59,69,89]

Zero-point corrected energies $[E(0)]$, energies including finite temperature corrections $[E(T)]$, enthalpies $[H(T)]$, and Gibbs free energies $[G(T)]$, were evaluated by combining the MP2/6-31+G* thermodynamic corrections with the RI-MP2/CBS electronic energies. Thermodynamic corrections are traditionally calculated from canonical partition functions with the assumption that the various degrees of freedom can be treated adequately using the ideal gas, rigid rotor, and harmonic oscillator (RRHO) approximations. The harmonic approximation of vibrational modes is considered problematic in the case of low frequency, large amplitude intermolecular modes of weakly bound systems. We have partially corrected for anharmonic behavior by scaling the harmonic ZPVE and thermodynamic corrections to match second-order vibrational perturbation theory (VPT2)[110] anharmonic values. For small water clusters and sulfuric acid monomer hydrates we have previously determined and applied multiplicative scaling factors for the ZPVE, $\Delta H_{\text{vib}}(T)$, and $S_{\text{vib}}(T)$ expressions using MP2/aVDZ.[59,89,90] The method is accurate enough that for the much studied water hexamer system,[111−114] we have been able to predict the three lowest lying isomers (Prism, Cage, and Book) at low temperature, and successfully show that the Book is the minimum at intermediate temperatures and that cyclic isomers dominate at temperatures higher than 200 K.[89,91,115,116]

dx.doi.org/10.1021/jp3054394 | J. Phys. Chem. A 2012, 116, 9745−9758

Table 1. RI-MP2/CBS//6-31+G* [a] Harmonic, Scaled Harmonic, and VPT2 Anharmonic $\Delta E(0K)$, $\Delta H(298.15K)$, and $\Delta G(298.15K)$ for Four Isomers of $(H_2SO_4)_2$ and $(H_2SO_4)_2(H_2O)$

	$\Delta E(0K)$			$\Delta H(298.15K)$			$\Delta G(298.15K)$		
$(H_2SO_4)_2$	harm.	anharm	sc harm.	harm.	anharm	sc harm.	harm.	anharm	sc harm.
I-a (C_1)	−16.58	−16.70	−16.82	−16.80	−16.87	−16.97	−5.33	−5.71	−6.02
I-b (C_1)	−15.67	−15.80	−15.91	−15.95	−16.04	−16.12	−4.36	−4.68	−5.06
I-c (C_i)	−16.07	−16.19	−16.31	−16.06	−16.15	−16.21	−6.03	−6.99	−6.84
I-d (C_2)	−15.80	−15.95	−16.04	−15.77	−15.87	−15.92	−5.38	−6.34	−6.20
	$\Delta E(0K)$			$\Delta H(298.15K)$			$\Delta G(298.15K)$		
$(H_2SO_4)_2(H_2O)$	harm.	anharm	sc harm.	harm.	anharm	sc harm.	harm.	anharm	sc harm.
I-a	−28.02	−28.38	−28.33	−28.89	−29.05	−29.03	−8.40	−9.51	−9.46
I-b	−27.55	−27.90	−27.86	−28.41	−28.60	−28.55	−7.98	−8.64	−9.04
I-c	−27.59	−27.98	−27.90	−28.50	−28.72	−28.64	−7.98	−9.26	−9.03
I-d	−26.96	−27.42	−27.27	−27.73	−27.93	−27.86	−7.65	−9.11	−8.74
MAE [b]	**0.26**		**0.09**	**0.15**		**0.07**	**0.89**		**0.25**

[a] Harm. = using harmonic frequencies; anharm = using VPT2 fundamental frequencies; sc harm. = using scaling factors for the ZPVE, $\Delta H_{vib}(298.15K)$ and $S_{vib}(298.15K)$ of 0.981, 1.053, and 1.095. [b] Mean absolute error relative to the anharmonic value.

Following that same procedure, here we calculated VPT2/MP2/6-31+G* fundamental frequencies for four $(H_2SO_4)_2$ and four $(H_2SO_4)_2(H_2O)$ isomers using Gaussian 09[99] with tight convergence criteria and small displacements (0.001 Å) used in the numerical calculation for cubic and semidiagonal quartic force constants. For $(H_2SO_4)_2(H_2O)_n$ clusters, we determined the optimal scaling factors for the ZPVE, $\Delta H_{vib}(216.65K)$, $\Delta H_{vib}(273.15K)$, $\Delta H_{vib}(298.15K)$, $S_{vib}(216.65K)$, $S_{vib}(273.15K)$, and $S_{vib}(298.15K)$ to be 0.981, 1.067, 1.056, 1.053, 1.116, 1.110, and 1.095, respectively. The harmonic and VPT2 fundamental frequencies are included in Tables S2−S7, Supporting Information.

Because of the small energetic differences, we have reported the binding and relative energies to the second decimal place to preserve information. The actual error bars in our methodology are expected to be less than 1 kcal mol^{-1} for electronic energies and up to 1−2 kcal mol^{-1} for free energies. We weighted the contribution of each low energy isomer by its Boltzmann factor to derive Boltzmann averaged enthalpies and free energies. The Boltzmann averaged free energies were combined with realistic estimates of sulfuric acid and water vapor concentrations in the troposphere to determine abundances of sulfuric acid monomer and dimer hydrates at equilibrium.[117] Standard state conditions are 1 atm pressure and the stated temperature. Molecular graphics are generated with Chimera 1.6 using the default hydrogen bond definitions.[118]

3. RESULTS

The 65 minima located in this study for $(H_2SO_4)_2(H_2O)_{n=0-6}$ are shown in Figures 1−7, in order of increasing electronic energy. The structures are labeled "I" if the cluster remains intact as $(H_2SO_4)_2(H_2O)_n$, "II" if one sulfuric acid undergoes a first acid dissociation to form $(H_2SO_4)(HSO_4^-H_3O^+)(H_2O)_{n-1}$, and "III" if both sulfuric acids undergo a first acid dissociation to form $(HSO_4^-H_3O^+)_2(H_2O)_{n-2}$. Table 1 contains energies based on harmonic, anharmonic, and scaled harmonic frequencies for four isomers of $(H_2SO_4)_2$ and four isomers of $(H_2SO_4)_2(H_2O)$. The $\Delta E°(0K)$, $\Delta H°(298.15K)$, and $\Delta G°(298.15K)$ energies for these 8 structures are always more negative when corrected for anharmonicity. The scaled harmonic values are much closer to the anharmonic values than to the harmonic values. Relative to the anharmonic values, the mean absolute error (MAE) of the harmonic and scaled harmonic analogs are 0.26 and 0.09 kcal mol^{-1} for $\Delta E°(0K)$, 0.15 and 0.07 kcal mol^{-1} for $\Delta H°(298.15K)$, and 0.89 and 0.25 kcal mol^{-1} for $\Delta G°(298.15K)$, respectively. Tables 2−6 display the RI-MP2/CBS//6-31+G* scaled harmonic binding electronic energies, enthalpies, and free energies for $(H_2SO_4)_2(H_2O)_{0-6}$ at 0, 216.65, 273.15, and 298.15 K. Table 7 contains the RI-MP2/CBS//6-31+G* Boltzmann averaged scaled harmonic binding energies for the formation of the sulfuric acid dimer hydrates displayed in the figures. Figure 8 shows the thermodynamics for adding water monomers to a $(H_2SO_4)_2(H_2O)_{n-1}$ cluster to form $(H_2SO_4)_2(H_2O)_n$ clusters and this process becomes thermodynamically unfavorable with increasing cluster size. However, the combination of sulfuric acid monomer hydrates to form dimer hydrates is substantially more favorable as illustrated in Figure 9. The dissociation of sulfuric acid into ion pairs occurs even in small gas-phase clusters such as the dimer hydrates investigated in this study. As Figure 10 demonstrates, the first acid dissociation of one of the sulfuric acids occurs in the presence of two waters at 0 K and three waters at 298.15 K. Both sulfuric acids of the dimer hydrate undergo first acid dissociation to two bisulfate anions and two hydronium cations in the presence of four waters at 0 K and five waters at 298.15 K. Figure 11 shows the equilibrium sulfuric acid monomer and dimer hydrate concentration at 20%, 50%, and 100% relative humidity, a sulfuric acid concentration of 5×10^7 molecules/cm^3, and three different temperatures of interest for atmospheric chemistry. The hydrate concentration shows little dependence on relative humidity and a significant variation with temperature. The concentration of $H_2SO_4(H_2O)_n$ typically exceeds that of $(H_2SO_4)_2(H_2O)_n$ by a few orders of magnitude for small n, but $(H_2SO_4)_2(H_2O)_n$ forms in significant numbers at low temperatures.

4. DISCUSSION

4.1. Anharmonicity Corrections. In the absence of complete experimental vibrational data, a common occurrence for most hydrogen bonded systems and these sulfuric acid dimer hydrates, we have used VPT2[110] anharmonic frequencies as a substitute. The water dimer is the only water cluster system where the vibrational spectrum is fully[87] resolved, and for this system VPT2 frequencies are very close to experiment.[87,119,120] We have derived accurate scaling factors for the harmonic

dx.doi.org/10.1021/jp3054394 | J. Phys. Chem. A 2012, 116, 9745−9758

frequencies, ZPVE and thermodynamic corrections for use on larger water clusters.[90] Thermodynamic corrections calculated using VPT2 frequencies agree better with experiment[121] and benchmark theory[122] for the dimerization energy of water. Spectroscopic studies of sulfuric acid have yielded insight on photolysis, vibrational, and electronic structure,[123−129] but the experimental spectra of it and its monohydrate[124] are incomplete and assignments are ambiguous. Therefore, we have used VPT2/MP2/aVDZ anharmonic frequencies as proxies for experimental frequencies, and to derive scaling factors for sulfuric acid monomer hydrates.[59] Others have used VSCF[130] to obtain fundamental frequencies.[131] Here, we use the VPT2/MP2/6-31+G* anharmonic ZPVE, vibrational enthalpy and entropy to derive scaling factors. The scaled harmonic ΔE(0K), ΔH(298.15K), and ΔG(298.15K) compare well with the anharmonic analogs as indicated by low MAE values in Table 1. The anharmonic correction is largest for the Gibbs free energy due to the large dependence of the entropy on the highly anharmonic low frequency vibrational modes.

4.2. Structures. Sulfuric acid has a dipole moment of 2.96 D;[132] the complex with water has dipole moments ranging from 2.6 to 3.0 D.[133] It has extremely strong interactions with other sulfuric acid monomers and with water,[134] making the search for all possible configurations of these complexes challenging. Although we cannot guarantee that we have found the global minimum in every set of isomers, we believe that we have widely sampled the RI-MP2 hypersurfaces and have located a compelling set of diverse structures for each set of clusters. Figure 1 shows that the sulfuric acid dimers, $(H_2SO_4)_2$, have

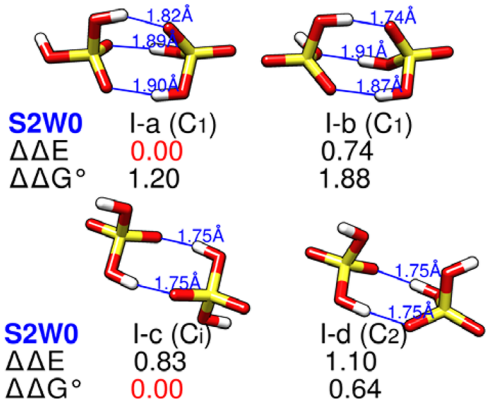

Figure 1. RI-MP2/CBS//6-31+G* low energy isomers of $(H_2SO_4)_2$ ordered by increasing $\Delta\Delta E$. $\Delta\Delta G°$ represents the relative free energy at a standard state of 298.15 K and 1 atm. The bond distances are in Angstroms.

four isomers in close energetic proximity. The first two isomers, I-a and I-b are composed of one *cis*- and one *trans*-H_2SO_4 and have C_1 symmetry. The I-c and I-d isomers are composed of two *trans*-H_2SO_4 monomers and have C_i and C_2 symmetry, respectively. The I-a (C_1) isomer has three strong hydrogen bonds, making it the electronic energy minimum. The I-b (C_1) dimer also has three hydrogen bonds, but one is a weaker O−H---O−H interaction, as opposed to the stronger O−H---O bonds found in I-a (C_1). The I-c (C_i) dimer, arranged in a trans−trans configuration, only has two strong hydrogen bonds and its higher entropy makes it the free energy minimum. The I-d (C_2) dimer also has two strong hydrogen bonds, but it is less stable than I-c (C_i) due to the proximity of the two free hydroxyl groups and its lower rotational entropy as a result of its C_2 spatial symmetry.

For $(H_2SO_4)_2(H_2O)$ hydrates, we located eight low-lying conformers. As shown in Figure 2, the I-a isomer has the lowest

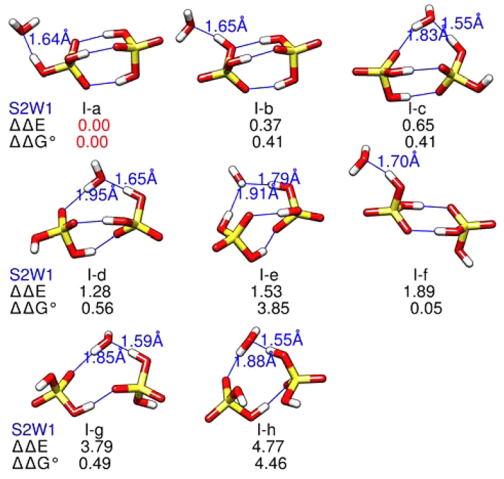

Figure 2. RI-MP2/CBS//6-31+G* low energy isomers of $(H_2SO_4)_2(H_2O)$ ordered increasing $\Delta\Delta E$. $\Delta\Delta G°$ represents the relative free energy at a standard state of 298.15 K and 1 atm.

electronic and free energy, although five of the next six conformers are within 0.6 kcal mol^{-1} of the free energy minimum and uncertainties in the scaled harmonic approximation make it impossible to claim for certain that I-a is the global free energy minimum. The I-a structure is based on the I-a (C_1) dimer (Figure 1), with water bound to the remaining free hydroxyl group (or acidic proton). The I-b isomer is based on the I-b (C_1) dimer, and the I-f isomer is based on the I-c (C_i) dimer (Figure 1); in these three structures a water serves as a hydrogen bond acceptor from a hydroxyl group of a sulfuric acid. The primary hydrogen bonds between the acidic proton of sulfuric acid and the acceptor water are strong in these structures, characterized by short hydrogen bond lengths and angles approaching linearity.[2] The remaining five isomers have the sulfuric acid dimer structure perturbed by a single donor-single acceptor (I-c, I-d, I-g, I-h) or double acceptor (I-e) water molecule bridging the two sulfuric acids. Overall, the addition of a water molecule to the sulfuric acid dimer allows the formation of one more outer or bridging hydrogen bond. With the exception of the I-e isomer, the additional hydrogen bond has a short distance (1.55−1.70 Å) compared to the hydrogen bonds in the unhydrated dimer.

Figure 3 displays the twelve $(H_2SO_4)_2(H_2O)_2$ isomers. Three of the lowest energy isomers are di-ionic structures. The lowest electronic energy structure is clearly the di-ionic isomer II-a in which the three bisulfate oxygens accept four hydrogen bonds from the sulfuric acid (two), the hydronium, and the water. In terms of free energy, however, the neutral structure I-c is the minimum energy structure, which can be thought of as the $(H_2SO_4)_2(H_2O)$ structure I-c with an extra water accepting a hydrogen bond from one of the sulfuric acid hydroxyl groups. Isomer I-f is 0.85 kcal mol^{-1} higher in free energy, and this structure consists of the $(H_2SO_4)_2$ dimer structure I-d (C_2), with two water molecules acting as hydrogen bond acceptors on either side of the sulfuric acid dimer structure. Structures I-c, I-f, and I-i allow for an interesting perspective on the methods used in this study. Structures I-f and I-i can be constructed from

dx.doi.org/10.1021/jp3054394 | J. Phys. Chem. A 2012, 116, 9745−9758

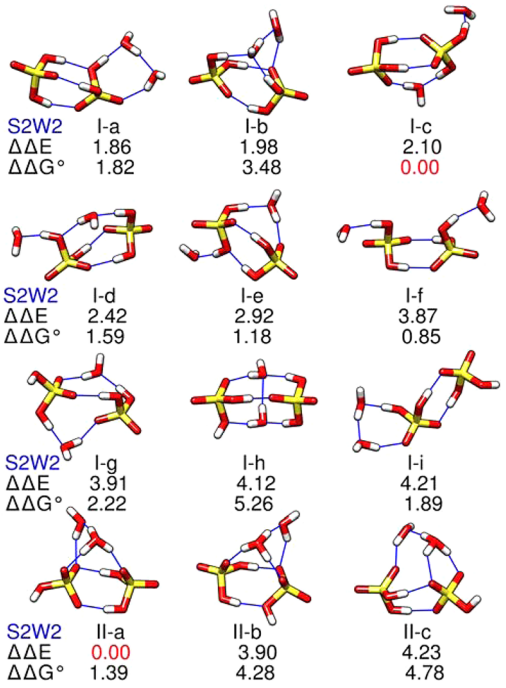

Figure 3. RI-MP2/CBS//6-31+G* low energy isomers of $(H_2SO_4)_2(H_2O)_2$ ordered by state of dissociation (I, II, III) and increasing $\Delta\Delta E$. $\Delta\Delta G°$ represents the relative free energy at a standard state of 298.15 K and 1 atm.

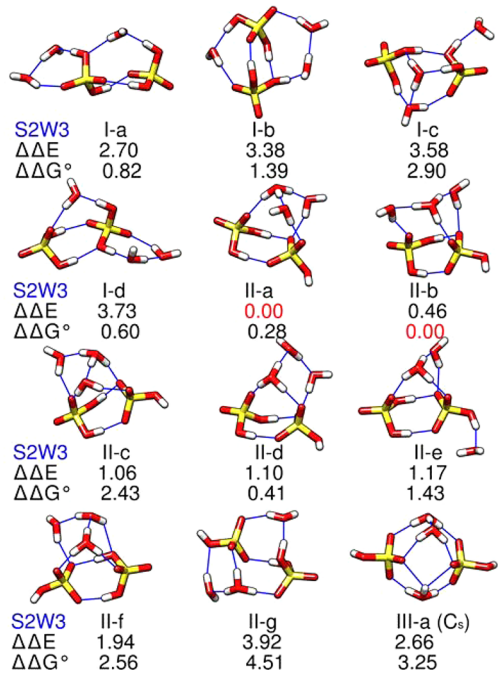

Figure 4. RI-MP2/CBS//6-31+G* low energy isomers of $(H_2SO_4)_2(H_2O)_3$ ordered by state of dissociation (I, II, III) and increasing $\Delta\Delta E$. $\Delta\Delta G°$ represents the relative free energy at a standard state of 298.15 K and 1 atm.

the $(H_2SO_4)_2$ dimers I-d (C_2) and I-c (C_i), simply by adding water molecules in obvious places, yet these two $(H_2SO_4)_2(H_2O)_2$ structures are both approximately 4 kcal mol^{-1} higher in electronic energy than the II-a minimum, and 1−2 kcal mol^{-1} higher than the I-c free energy minimum.

The twelve lowest energy structures for the $(H_2SO_4)_2(H_2O)_3$ cluster are displayed in Figure 4. Four of the lowest energy structures are neutral, seven are di-ionic, and one (III-a) is tetra-ionic, meaning that both sulfuric acid molecules have dissociated to two bisulfate and two hydronium ions. The neutral and di-ionic structures (except II-c) have a network of seven hydrogen bonds and the tetra-ionic structure (III-a) has a network of nine hydrogen bonds. Structures II-a and II-b are the most stable in terms of electronic and free energy at 298.15 K, respectively. In both isomers, the water−hydronium−water hydrogen bonding network and the remaining sulfuric acid all donate hydrogen bonds to the bisulfate anion. Unlike the neutral structures where the waters are equally likely to form bridging or outer hydrogen bonds, the hydronium in the di-ionic isomers favors the formation of bridging structures where the hydronium ion donates three hydrogen bonds. The tetra-ionic structure III-a, although much higher in energy than the minimum, illustrates a new structural motif that emerges as more waters are added. In this isomer, the hydroniums and the water are inserted between the bisulfates, bridging the two anions. There are no hydrogen bonds between the bisulfates and this configuration provides charge separation thereby minimizing the electrostatic repulsion between the bisulfate anions as well as the hydroniums. Also, even though the bisulfate ion, the hydronium ion and water each have large dipole moments of their own, they mostly cancel each other out leading to a much smaller electric dipole moment for the tetra-ionic isomer compared to those of the neutral and di-ionic clusters. The electric dipole moment for all species is provided in Table S14, Supporting Information. The symmetric C_s tetra-ionic structure has nine hydrogen bonds and correspondingly lower entropy than the neutral and di-ionic isomers. Thus, it is more favorable energetically than it is entropically: $\Delta\Delta E < \Delta\Delta G°$.

For the $(H_2SO_4)_2(H_2O)_4$ system, we found the two neutral, six di-ionic, and six tetra-ionic isomers shown in Figure 5. The tetra-ionic structure III-a is the lowest electronic energy isomer and there is no other isomer within 1 kcal mol^{-1}. Similar to the III-a isomer of $(H_2SO_4)_2(H_2O)_3$, the hydroniums and waters bridge the two bisulfates in the 10 hydrogen bond network of the III-a isomer. With the exception of the III-f structure, all the tetra-ionic isomers have a notable spatial symmetry and a small dipole moment (0.00−2.85 D) compared to that of neutral and di-ionic clusters (3.71−7.59 D). The di-ionic structure II-b is the lowest free energy structure. Here the neutral sulfuric acid donates two hydrogen bonds to the bisulfate, and the three waters and the hydronium form a network bridging the dimer structure. Overall II-b has a network of nine hydrogen bonds. The neutral isomers, I-a and I-b are very unfavorable, with their electronic energy lying more than 6 kcal mol^{-1} above the global minimum. The typical distance between the two sulfurs for the low energy structures is around 4 Å for the neutral and di-ionic clusters but increases to about 5 Å for the tetra-ionic isomers. This increase can be attributed to the repulsion between the like-charged ions even though recent publications on monovalent ions indicate that like-charged ions in aqueous solution can actually attract each other strongly if their charge density is large such as for fluoride ions.[135] The ions in our $(HSO_4^-)_2(H_3O^+)_2(H_2O)_{n-2}$ have low charge density and the net interaction between the like-charged ions should be repulsive.

The seven lowest energy isomers for the $(H_2SO_4)_2(H_2O)_5$ system are displayed in Figure 6. The lowest energy structures are now the tetra-ionic moieties III-a (electronic) and III-c (free

dx.doi.org/10.1021/jp3054394 | J. Phys. Chem. A 2012, 116, 9745−9758

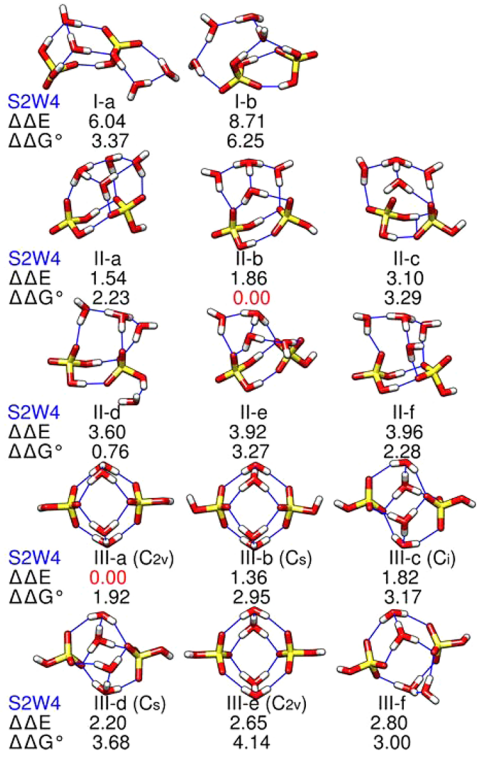

Figure 5. RI-MP2/CBS//6-31+G* low energy isomers of $(H_2SO_4)_2(H_2O)_4$ ordered by state of dissociation (I, II, III) and increasing $\Delta\Delta E$. $\Delta\Delta G°$ represents the relative free energy at a standard state of 298.15 K and 1 atm.

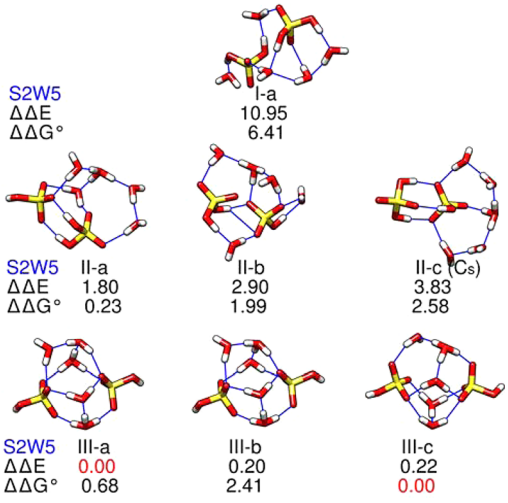

Figure 6. RI-MP2/CBS//6-31+G* low energy isomers of $(H_2SO_4)_2(H_2O)_5$ ordered by state of dissociation (I, II, III) and increasing $\Delta\Delta E$. $\Delta\Delta G°$ represents the relative free energy at a standard state of 298.15 K and 1 atm.

energy), each containing a network of 11 hydrogen bonds. Continuing the trend found with $(H_2SO_4)_2(H_2O)_{3-4}$, the bisulfate anions are separated by the hydronium ions and waters, leading to a symmetric structure that is very favorable energetically. In terms of electronic energy, the most stable di-ionic and neutral isomers are 1.80 and 10.95 kcal mol^{-1} higher, respectively, but they are only 0.23 and 6.41 kcal mol^{-1} higher in terms of $G°(298.15K)$. Figure 7 displays the eight low energy isomers for the $(H_2SO_4)_2(H_2O)_6$ cluster. The electronic and

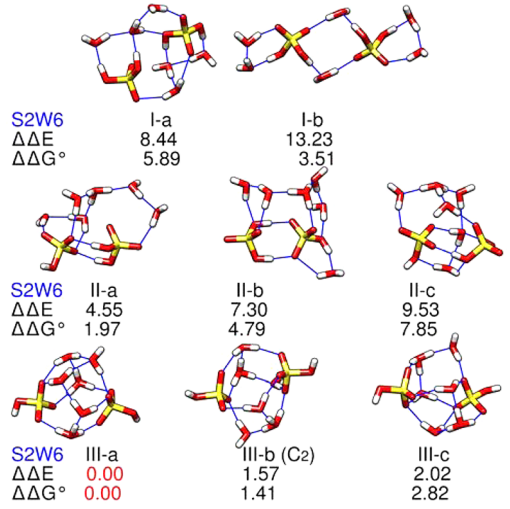

Figure 7. RI-MP2/CBS//6-31+G* low energy isomers of $(H_2SO_4)_2(H_2O)_6$ ordered by state of dissociation (I, II, III) and increasing $\Delta\Delta E$. $\Delta\Delta G°$ represents the relative free energy at a standard state of 298.15 K and 1 atm.

free energy minimum is the tetra-ionic structure III-a, which is a globular structure with the hydrogen-bonding network spanning the outside of this cluster. The other two structures within a kcal mol^{-1} of electronic or free energy are the III-b tetra-ionic structure and the II-c di-ionic structure. Ring formation is a known dominant motif in multiply hydrated acid complexes,[2] and the sulfuric acid clusters reported in this study form closed rings.

4.3. Acid Dissociation. Water catalyzes and mediates a lot of processes including acid dissociation.[136] The dissociation of a hydrated sulfuric acid moiety into hydrated ionic species is one of the most interesting features of sulfuric acid hydrates. As a strong acid, sulfuric acid completely dissociates in aqueous solutions, and deprotonation in the gas phase happens in the presence of a few waters. Numerous researchers have predicted the gas-phase deprotonation of a single H_2SO_4 to occur at different cluster sizes depending on the temperature and the level of theory employed.[51−55,137] Leopold's recent review of hydrated acid clusters made the point that strong monoprotic acids typically need three to five water molecules before the lowest energy complex contains the ionized acid.[2] He notes that the relative stability of the neutral and ionized species depends on a delicate balance between proton transfer energy, Coulombic attraction, and hydrogen-bond stabilization.[2] Our calculations on $H_2SO_4(H_2O)_{n=1-6}$ predict that the ionic pair clusters become the global minima in terms of E_e and $G(298.15K)$ when $n \geq 4$ and $n = 6$, respectively.[59]

Acid dissociation at a molecular level has been of great interest. Recent experimental works on the aggregation-induced acid dissociation of $HCl(H_2O)_n$[138−140] suggest a mechanism for the proton transfer process. Bianco and Hynes studied the H_2SO_4 first acid dissociation on the surface of aqueous aerosols using theoretical methods.[141,142] For $(H_2SO_4)_2(H_2O)_n$ clusters, Ding et al.'s DFT work predicted ion pair formation to occur in the presence of two or more waters.[98] The present work agrees with the previous prediction. Our results provide a picture of the first deprotonation of sulfuric acid as a function of temperature for a system consisting of two sulfuric acid molecules and up to six waters (Figure 10). At 0 K, a cluster of two sulfuric acid molecules and a single water remain

dx.doi.org/10.1021/jp3054394 | J. Phys. Chem. A 2012, 116, 9745−9758

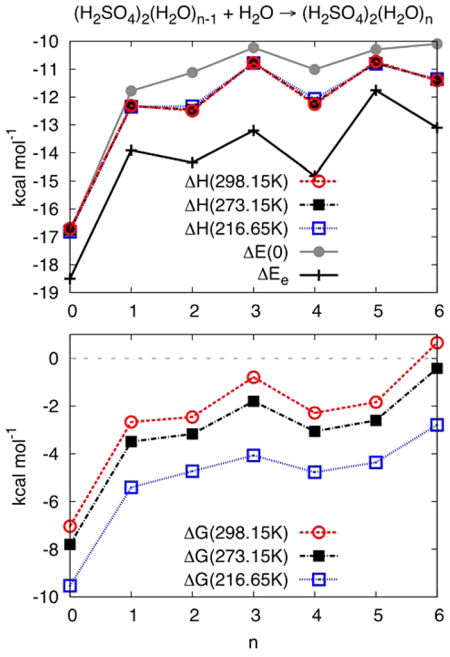

Figure 8. RI-MP2/CBS//6-31+G* Boltzmann averaged scaled harmonic thermodynamics of stepwise $[(H_2SO_4)_2(H_2O)_{n-1} + H_2O \rightarrow (H_2SO_4)_2(H_2O)_n]$ sulfuric acid dimer hydrate growth. $n = 0$ corresponds to $2(H_2SO_4) \rightarrow (H_2SO_4)_2$.

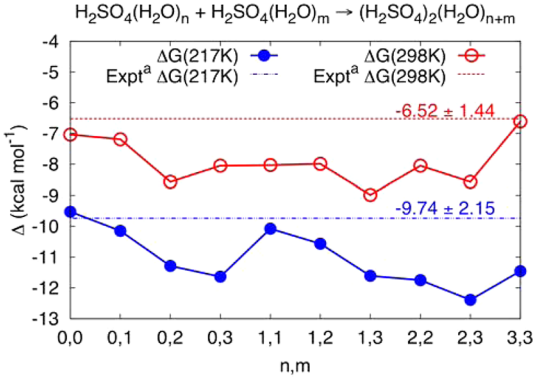

Figure 9. RI-MP2/CBS//6-31+G* scaled harmonic thermodynamics for $H_2SO_4(H_2O)_n + H_2SO_4(H_2O)_m \rightarrow (H_2SO_4)_2(H_2O)_{n+m}$. Expt[a]: Experimental free energy of forming H_2SO_4 dimer hydrates from H_2SO_4 monomer hydrates averaged over all hydrates from ref 148.

undissociated. Addition of a second water results in deprotonation of most of the clusters, with the di-ionic species more stable than completely neutral moieties. Upon the addition of a third water molecule, the second sulfuric acid molecule begins to dissociate. For the $(H_2SO_4)_2(H_2O)_3$ cluster, the di-ionic cluster is a few kcal mol^{-1} more stable than the neutral cluster, which is just slightly more stable than the tetra-ionic cluster (Figure 10, top right). The tetra-ionic cluster, $(HSO_4^-)_2(H_3O^+)_2(H_2O)_2$, becomes as favorable as the di-ionic cluster $H_2SO_4(HSO_4^-)(H_3O^+)(H_2O)_3$, for a cluster of two sulfuric acid molecules and four waters at 0 K. Increasing temperature does not change the start of dissociation but does favor the undissociated clusters, and at room temperature we predict that the di-ionic species is slightly more favorable than the neutral cluster once three waters have been added to the cluster. The tetra-ionic species competes with the di-ionic species once five waters have been added to the cluster (Figure

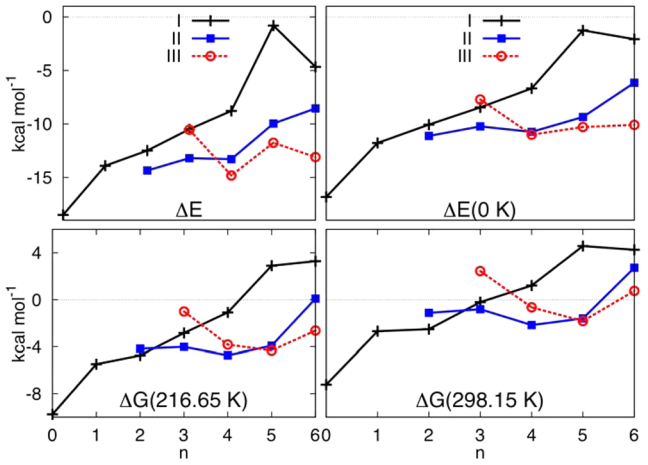

Figure 10. RI-MP2/CBS//6-31+G* scaled harmonic thermodynamics of stepwise $[(H_2SO_4)_2(H_2O)_{n-1} + H_2O \rightarrow (H_2SO_4)_2(H_2O)_n]$ sulfuric acid hydrate growth of the neutral (I), di-ionic (II) and tetra-ionic(III) isomers. The change in energy is defined as the difference between the Boltzmann averaged value for the nth cluster of a particular state (I, II, III) and $(n-1)$th cluster of all states. $n = 0$ corresponds to $2(H_2SO_4) \rightarrow (H_2SO_4)_2$.

10, bottom right). The finding that two sulfuric acids begin to dissociate in the presence of fewer waters than does a single sulfuric acid may have important implications for solutions of concentrated sulfuric acid. Because the relative acidity of a cluster increases with the number of sulfuric acid monomers present, it makes sense that fewer waters are needed to cause the acid dissociation. We tentatively predict that less water is necessary for acid dissociation to begin when more sulfuric acid molecules are present.

4.4. Thermodynamics of $(H_2SO_4)_2(H_2O)_n$ Formation.

The structure and thermodynamics of $(H_2SO_4)_2(H_2O)_n$ have been investigated using various density functional methods [B3LYP/6-311++G(2d,2p),[143] PW91/DNP,[9856] and PW91/6-311++G(3df,3pd)[144]] and wave function methods [RI-MP2/aV(T+d)Z//MPW1B95/aV(D+d)Z[145] and RI-MP2/def2-QZVPP[146]]. Most of these studies focused on $(H_2SO_4)_2(H_2O)_{n=0-2}$, and the PW91/DNP work by Ding et al.[98] is unique in that it explores $(H_2SO_4)_2(H_2O)_{n=0-8}$ and the role of acid dissociation that emerges for $n \geq 2$.

Tables 2−6 contain the scaled harmonic binding energies, enthalpies, and free energies for the $(H_2SO_4)_2(H_2O)_{n=0-6}$ clusters, with the single point energies computed with the aug-cc-pVDZ, aug-cc-pVTZ, and aug-cc-pVQZ basis sets and extrapolated using eq 1 before the inclusion of the scaled harmonic thermodynamic corrections as described in the Methodology and footnoted in the tables. The dimerization of sulfuric acid is exothermic by 16−17 kcal mol^{-1}, and the formation of a cluster containing two sulfuric acids and a water is exothermic by 27−29 kcal mol^{-1}. For a cluster containing two sulfuric acids and six waters, 74−84 kcal mol^{-1} is released. Free energies are lower, but still largely negative, ranging from −7 kcal mol^{-1} for dimerization of sulfuric acid, to −10 kcal mol^{-1} for the formation of the $(H_2SO_4)_2(H_2O)$ cluster, to −12 kcal mol^{-1} for the $(H_2SO_4)_2(H_2O)_2$ cluster, to −13 kcal mol^{-1} for the $(H_2SO_4)_2(H_2O)_3$ cluster, to −15 kcal mol^{-1} for the $(H_2SO_4)_2(H_2O)_4$ cluster, to −17 kcal mol^{-1} for the $(H_2SO_4)_2(H_2O)_5$ cluster, to −17 kcal mol^{-1} for the $(H_2SO_4)_2(H_2O)_6$ cluster, all at room temperature. These values are in good agreement with previous results by Torpo

dx.doi.org/10.1021/jp3054394 | J. Phys. Chem. A 2012, 116, 9745−9758

Table 2. RI-MP2/CBS//6-31+G* [a] Scaled Harmonic[b] Binding Energies for $(H_2SO_4)_2(H_2O)_{n=0-1}$[c]

		CBS	0 K	216.65 K		273.15 K		298.15 K	
n	isomer	ΔE_e[MP2]	ΔE	ΔH	ΔG	ΔH	ΔG	ΔH	ΔG
0	I-a(C_1)	**−18.50**	**−16.82**	**−17.08**	−8.98	**−17.02**	−6.89	**−16.98**	−5.97
0	I-b(C_1)	−17.75	−16.12	−16.40	−8.31	−16.34	−6.21	−16.31	−5.29
0	I-c(C_i)	−17.67	−16.52	−16.52	**−9.71**	−16.44	**−7.94**	−16.39	**−7.16**
0	I-d(C_2)	−17.40	−16.25	−16.24	−9.17	−16.15	−7.33	−16.10	−6.52
1	I-a	**−32.40**	**−28.60**	**−29.41**	**−15.24**	**−29.32**	**−11.54**	**−29.26**	**−9.92**
1	I-b	−32.04	−28.13	−28.93	−14.81	−28.84	−11.13	−28.78	−9.51
1	I-c	−31.75	−28.17	−29.00	−14.83	−28.93	−11.13	−28.87	−9.50
1	I-d	−31.12	−27.55	−28.27	−14.52	−28.16	−10.93	−28.09	−9.35
1	I-e	−30.88	−26.08	−27.21	−11.83	−27.18	−7.84	−27.15	−6.07
1	I-f	−30.51	−27.05	−27.58	−14.71	−27.46	−11.35	−27.38	−9.87
1	I-g	−28.62	−25.48	−25.94	−13.96	−25.80	−10.81	−25.72	−9.43
1	I-h	−27.63	−24.48	−25.20	−10.83	−25.06	−7.10	−24.98	−5.46

[a]RI-MP2/aVDZ//6-31+G*, RI-MP2/aVTZ//6-31+G*, RI-MP2/aVQZ//6-31+G* binding energies extrapolated using eq 1. [b]ZPVE, ΔH_{vib}(216.65K), ΔH_{vib}(273.15K), ΔH_{vib}(298.15K), S_{vib}(216.65K), S_{vib}(273.15K), and S_{vib}(298.15K) scaled by 0.981, 1.067, 1.056, 1.053, 1.116, 1.110, and 1.095, respectively. [c]All energies are in kcal mol^{-1}. Global minima shown in bold.

Table 3. RI-MP2/CBS//6-31+G* [a] Scaled Harmonic[b] Binding Energies for $(H_2SO_4)_2(H_2O)_{n=2}$[c]

		CBS	0 K	216.65 K		273.15 K		298.15 K	
n	isomer	ΔE_e[MP2]	ΔE	ΔH	ΔG	ΔH	ΔG	ΔH	ΔG
2	I-a	−44.90	−38.24	−39.91	−18.63	−39.85	−13.08	−39.79	−10.62
2	I-b	−44.77	−37.42	−39.27	−17.24	−39.24	−11.49	−39.20	−8.96
2	I-c	−44.65	−38.66	−39.98	**−19.98**	−39.87	**−14.75**	−39.79	**−12.44**
2	I-d	−44.33	−37.79	−39.18	−18.60	−39.07	−13.22	−38.99	−10.85
2	I-e	−43.83	−37.77	−39.12	−18.88	−39.00	−13.59	−38.92	−11.26
2	I-f	−42.88	−37.06	−38.13	−18.86	−37.96	−13.81	−37.86	−11.59
2	I-g	−42.84	−36.86	−38.24	−17.89	−38.13	−12.57	−38.04	−10.22
2	I-h	−42.64	−35.35	−37.07	−15.34	−37.01	−9.68	−36.95	−7.18
2	I-i	−42.54	−36.36	−37.65	−17.97	−37.53	−12.82	−37.44	−10.55
2	II-a	**−46.75**	**-39.72**	**−41.60**	−19.41	**−41.61**	−13.61	**−41.59**	−11.05
2	II-b	−42.86	−36.07	−37.79	−16.27	−37.77	−10.65	−37.73	−8.16
2	II-c	−42.52	−35.56	−37.39	−15.80	−37.40	−10.16	−37.37	−7.66

[a]RI-MP2/aVDZ//6-31+G*, RI-MP2/aVTZ//6-31+G*, RI-MP2/aVQZ//6-31+G* binding energies extrapolated using eq 1. [b]ZPVE, ΔH_{vib}(216.65K), ΔH_{vib}(273.15K), ΔH_{vib}(298.15K), S_{vib}(216.65K), S_{vib}(273.15K), and S_{vib}(298.15K) scaled by 0.981, 1.067, 1.056, 1.053, 1.116, 1.110, and 1.095, respectively. [c]All energies are in kcal mol^{-1}. Global minima shown in bold.

Table 4. RI-MP2/CBS//6-31+G* [a] Scaled Harmonic[b] Binding Energies for $(H_2SO_4)_2(H_2O)_{n=3}$[c]

		CBS	0 K	216.65 K		273.15 K		298.15 K	
n	isomer	ΔE_e[MP2]	ΔE	ΔH	ΔG	ΔH	ΔG	ΔH	ΔG
3	I-a	−57.25	−48.16	−50.38	−22.82	−50.29	−15.61	−50.21	−12.43
3	I-b	−56.57	−47.97	−50.17	−22.34	−50.07	−15.07	−49.97	−11.87
3	I-c	−56.37	−46.65	−48.95	−20.91	−48.87	−13.59	−48.78	−10.36
3	I-d	−56.22	−47.55	−49.60	−22.77	−49.48	−15.75	−49.38	−12.65
3	II-a	**−59.95**	−49.82	−52.43	−23.79	**−52.49**	−16.29	**−52.46**	−12.98
3	II-b	−59.49	**−49.95**	**−52.47**	**−24.00**	−52.48	**−16.55**	−52.44	**−13.26**
3	II-c	−58.89	−48.81	−51.48	−21.95	−51.51	−14.24	−51.48	−10.83
3	II-d	−58.85	−49.29	−51.78	−23.52	−51.80	−16.12	−51.76	−12.85
3	II-e	−58.78	−48.92	−51.51	−22.69	−51.52	−15.16	−51.48	−11.83
3	II-f	−58.01	−48.26	−50.85	−21.69	−50.88	−14.07	−50.85	−10.70
3	II-g	−56.03	−46.43	−49.01	−19.76	−49.01	−12.13	−48.97	−8.75
3	III-a	−57.29	−47.43	−50.10	−20.99	−50.19	−13.38	−50.19	−10.00

[a]RI-MP2/aVDZ//6-31+G*, RI-MP2/aVTZ//6-31+G*, RI-MP2/aVQZ//6-31+G* binding energies extrapolated using eq 1. [b]ZPVE, ΔH_{vib}(216.65K), ΔH_{vib}(273.15K), ΔH_{vib}(298.15K), S_{vib}(216.65K), S_{vib}(273.15K), and S_{vib}(298.15K) scaled by 0.981, 1.067, 1.056, 1.053, 1.116, 1.110, and 1.095, respectively. [c]All energies are in kcal mol^{-1}. Global minima shown in bold.

et al.[145] employing the comparable RI-MP2/aV(T+d)Z//MPW1B95/aV(D+d)Z method for $(H_2SO_4)_2(H_2O)_{n=0-2}$ and another work by Salonen et al.[146] using the RI-MP2/QZVPP method for selected isomers of $(H_2SO_4)_2(H_2O)_{n=0-1}$. There is, however, a significant disagreement with results based on density functional methods. Although an earlier B3LYP/6-311+

dx.doi.org/10.1021/jp3054394 | J. Phys. Chem. A 2012, 116, 9745−9758

Table 5. RI-MP2/CBS//6-31+G* [a] Scaled Harmonic[b] Binding Energies for $(H_2SO_4)_2(H_2O)_{n=4}$[c]

		CBS	0 K	216.65 K		273.15 K		298.15 K	
n	isomer	ΔE_e[MP2]	ΔE	ΔH	ΔG	ΔH	ΔG	ΔH	ΔG
4	I-a	−68.73	−56.63	−59.65	−25.08	−59.57	−16.04	−59.47	−12.05
4	I-b	−66.06	−54.48	−57.49	−22.39	−57.39	−13.22	−57.29	−9.17
4	II-a	−73.23	−59.62	−63.17	−26.89	−63.27	−17.40	−63.25	−13.19
4	II-b	−72.91	−60.69	−63.95	**−28.73**	−63.99	**−19.50**	−63.95	**−15.43**
4	II-c	−71.67	−59.08	−62.42	−25.89	−62.42	−16.36	−62.36	−12.14
4	II-d	−71.17	−59.14	−62.28	−27.72	−62.28	−18.67	−62.22	−14.67
4	II-e	−70.85	−58.47	−61.80	−25.74	−61.82	−16.32	−61.77	−12.15
4	II-f	−70.81	−58.08	−61.28	−26.34	−61.31	−17.19	−61.26	−13.14
4	III-a	**−74.77**	**−60.96**	**−64.63**	−27.53	**−64.80**	−17.81	**−64.82**	−13.51
4	III-b	−73.41	−59.77	−63.51	−26.46	−63.69	−16.77	−63.70	−12.47
4	III-c	−72.95	−59.51	−63.16	−26.21	−63.32	−16.54	−63.32	−12.26
4	III-d	−72.57	−59.11	−62.79	−25.74	−62.95	−16.05	−62.96	−11.75
4	III-e	−72.12	−58.87	−62.58	−25.35	−62.77	−15.61	−62.79	−11.29
4	III-f	−71.97	−58.91	−62.43	−26.14	−62.56	−16.64	−62.55	−12.43

[a]RI-MP2/aVDZ//6-31+G*, RI-MP2/aVTZ//6-31+G*, RI-MP2/aVQZ//6-31+G* binding energies extrapolated using eq 1. [b]ZPVE, ΔH_{vib}(216.65K), ΔH_{vib}(273.15K), ΔH_{vib}(298.15K), S_{vib}(216.65K), S_{vib}(273.15K), and S_{vib}(298.15K) scaled by 0.981, 1.067, 1.056, 1.053, 1.116, 1.110, and 1.095, respectively. [c]All energies are in kcal mol^{-1}. Global minima shown in bold.

Table 6. RI-MP2/CBS//6-31+G* [a] Scaled Harmonic[b] Binding Energies for $(H_2SO_4)_2(H_2O)_{n=5\text{-}6}$[c]

		CBS	0 K	216.65 K		273.15 K		298.15 K	
n	isomer	ΔE_e[MP2]	ΔE	ΔH	ΔG	ΔH	ΔG	ΔH	ΔG
5	I-a	−75.57	−62.20	−65.52	−25.83	−65.33	−15.43	−65.18	−10.85
5	II-a	−84.73	−70.31	−74.04	−32.65	−74.00	−21.81	−73.91	−17.02
5	II-b	−83.63	−69.35	−73.26	−31.16	−73.25	−20.14	−73.17	−15.27
5	II-c	−82.69	−68.01	−71.86	−30.36	−71.84	−19.49	−71.76	−14.68
5	III-a	**−86.53**	**−71.24**	**−75.39**	−32.71	**−75.52**	−21.53	**−75.50**	−16.57
5	III-b	−86.33	−70.16	−74.50	−31.22	−74.68	−19.88	−74.68	−14.85
5	III-c	−86.31	−70.56	−74.77	**−33.06**	−74.92	**−22.11**	−74.92	**−17.26**
6	I-a	−91.18	−73.31	−77.91	−29.05	−77.86	−16.27	−77.75	−10.62
6	I-b	−86.40	−70.43	−74.12	−29.78	−73.90	−18.13	−73.73	−13.00
6	II-a	−95.08	−77.40	−81.87	−32.97	−81.81	−20.18	−81.69	−14.53
6	II-b	−92.33	−74.64	−79.20	−30.20	−79.16	−17.38	−79.05	−11.71
6	II-c	−90.10	−72.08	−76.71	−27.29	−76.67	−14.37	−76.56	−8.66
6	III-a	**−99.63**	**−81.33**	**−86.52**	**−35.71**	**−86.71**	**−22.40**	**−86.70**	**−16.51**
6	III-b	−98.06	−79.29	−84.32	−34.10	−84.51	−20.93	−84.50	−15.10
6	III-c	−97.60	−78.35	−83.54	−32.84	−83.74	−19.56	−83.73	−13.68

[a]RI-MP2/aVDZ//6-31+G*, RI-MP2/aVTZ//6-31+G*, RI-MP2/aVQZ//6-31+G* binding energies extrapolated using eq 1. [b]ZPVE, ΔH_{vib}(216.65K), ΔH_{vib}(273.15K), ΔH_{vib}(298.15K), S_{vib}(216.65K), S_{vib}(273.15K), and S_{vib}(298.15K) scaled by 0.981, 1.067, 1.056, 1.053, 1.116, 1.110, and 1.095, respectively. [c]All energies are in kcal mol^{-1}. Global minima shown in bold.

+G(2d,2p) work[143] underestimates the binding energy of the sulfuric acid dimer hydrates due to its failure to account for acid dissociation, studies employing PW91/DNP[56,98] predict stronger binding compared to our work.

Table 7 contains the Boltzmann averaged energies, both for the overall formation of each cluster (top) and for the stepwise hydration of each cluster (bottom). At 217 K, the temperature at the top of the troposphere, the free energies range from −10 kcal mol^{-1} for dimerization to −36 kcal mol^{-1} for formation of the $(H_2SO_4)_2(H_2O)_6$ cluster. Clearly, the thermodynamics favor formation of these structures. All of the stepwise free energies are negative, except for the formation of $(H_2SO_4)_2(H_2O)_6$ from $(H_2SO_4)_2(H_2O)_5$ and a sixth water, at T = 298 K. These results are shown graphically in Figure 8. The formation of the $(H_2SO_4)_2(H_2O)_4$ cluster appears to be particularly favorable, as the ensemble of the electronic energy minima dip to a minimum in the stepwise hydration. Clusters with n = 2, 4, 5 are clearly favored by free energy at all three temperatures.

The relative electronic energies at 0 K, and Gibbs free energies at 217 and 298 K for neutral (I), di-ionic (II), and tetra-ionic (III) sulfuric acid dimer hydrates under standard state conditions are illustrated in Figure 10. The figure demonstrates that the undissociated dimer hydrates (I) are the most stable clusters for n = 0−1, whereas both neutral and di-ionic clusters are found within 2 kcal mol^{-1} of the global minimum for n = 2−3. For n > 3, all the clusters within 2 kcal mol^{-1} of the global minimum were either di-ionic or tetra-ionic. The di-ionic and tetra-ionic structures are more strongly bound and hence have lower entropy. Thus, they become less favorable with increasing temperature, but they remain the global minima up to 298.15 K for $n \geq 3$.

4.5. Abundance of $(H_2SO_4)_{1-2}(H_2O)_n$ at Ambient Conditions. The concentration of a given cluster in the atmosphere can be estimated from the thermodynamics of

dx.doi.org/10.1021/jp3054394 | J. Phys. Chem. A 2012, 116, 9745−9758

Table 7. RI-MP2/CBS//6-31+G* [a] Boltzmann Averaged Scaled Harmonic[b] Binding Energy of Sulfuric Acid Hydrates[c]

	CBS	0 K	216.65 K		273.15 K		298.15 K	
n	ΔE_e[MP2]	ΔE	ΔH	ΔG	ΔH	ΔG	ΔH	ΔG
			$2(H_2SO_4) + n(H_2O) \rightarrow (H_2SO_4)_2(H_2O)_n$					
0	−18.50	−16.82	−16.82	−9.53	−16.75	−7.80	−16.71	−7.04
1	−32.40	−28.60	−29.17	−14.94	−29.08	−11.29	−29.02	−9.71
2	−46.75	−39.72	−41.50	−19.67	−41.53	−14.46	−41.51	−12.17
3	−59.95	−49.95	−52.27	−23.74	−52.31	−16.26	−52.28	−12.96
4	−74.77	−60.96	−64.34	−28.53	−64.52	−19.34	−64.54	−15.27
5	−86.53	−71.24	−75.15	−32.87	−75.29	−21.92	−75.27	−17.09
6	−99.63	−81.33	−86.50	−35.66	−86.69	−22.34	−86.68	−16.43
			$(H_2SO_4)_2(H_2O)_{n-1} + H_2O \rightarrow (H_2SO_4)_2(H_2O)_n$					
	−18.50	−16.82	−16.82	−9.53	−16.75	−7.80	−16.71	−7.04
1	−13.91	−11.78	−12.35	−5.41	−12.33	−3.49	−12.31	−2.67
2	−14.35	−11.12	−12.33	−4.73	−12.45	−3.17	−12.49	−2.46
3	−13.20	−10.23	−10.78	−4.07	−10.78	−1.80	−10.77	−0.79
4	−14.82	−11.01	−12.06	−4.79	−12.21	−3.08	−12.26	−2.30
5	−11.76	−10.29	−10.81	−4.34	−10.77	−2.58	−10.73	−1.82
6	−13.10	−10.09	−11.35	−2.79	−11.40	−0.42	−11.41	0.65

[a]RI-MP2/aVDZ//6-31+G*, RI-MP2/aVTZ//6-31+G*, RI-MP2/aVQZ//6-31+G* binding energies extrapolated using eq 1. [b]ZPVE, ΔH_{vib}(216.65K), ΔH_{vib}(273.15K), ΔH_{vib}(298.15K), S_{vib}(216.65K), S_{vib}(273.15K), and S_{vib}(298.15K) scaled by 0.981, 1.067, 1.056, 1.053, 1.116, 1.110, and 1.095, respectively. [c]All energies are in kcal mol^{-1}.

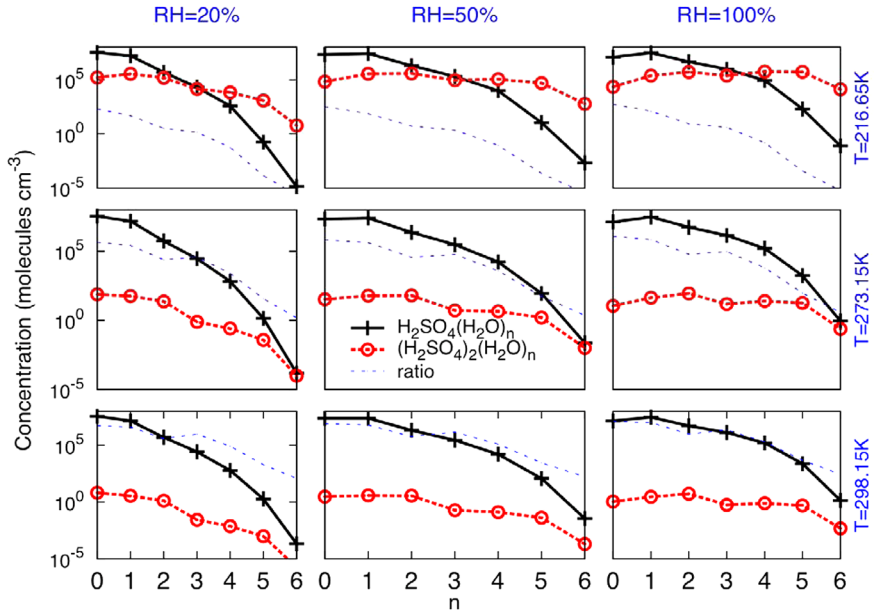

Figure 11. Equilibrium sulfuric acid monomer hydrate $[H_2SO_4(H_2O)_n]$ and dimer hydrate $[(H_2SO_4)_2(H_2O)_n]$ distribution assuming a saturation (100% RH) vapor pressure of $[H_2O] = 9.9 \times 10^{14}$, 1.6×10^{17}, and 7.7×10^{17} molecules/cm^3 at T = 216.65, 273.15, and 298.15 K, respectively, and $[H_2SO_4]_0 = 5 \times 10^7$ molecules/cm^3. Please note the logarithmic scale on the y-axis. The "ratio" represents $[H_2SO_4(H_2O)_n]$:$[(H_2SO_4)_2(H_2O)_n]$.

stepwise addition of a water molecule to each $(H_2SO_4)_2(H_2O)_{n-1}$ cluster to form $(H_2SO_4)_2(H_2O)_n$. The concentration of each successive hydrate depends on the concentration of the precursor $(H_2SO_4)_2(H_2O)_{n-1}$ hydrate, the concentration of water, and the stepwise thermodynamics presented in Figure 8. Assuming a closed system, and initial concentrations, one can solve for all of the equilibrium equations for the system. Using the RI-MP2/CBS//6-31+G* scaled harmonic free energies reported in Table 7, we calculated the concentration of $H_2SO_4(H_2O)_n$ and $(H_2SO_4)_2(H_2O)_n$ with a standard state of 1 atm and T = 216.65, 273.15, and 298.15 K for n = 0−6 waters. The saturation vapor pressure of water vapor corresponds to a number concentration of 9.9×10^{14}, 1.6×10^{17}, and 7.7×10^{17} cm^{-3} at the three temperatures.[6] The concentration of sulfuric acid vapor in the atmosphere typically ranges from 10^5−10^8 cm^{-3} on the basis of location and other factors.[21] We used a sulfuric acid concentration of 5×10^7 cm^{-3} because a concentration above ~10^7 cm^{-3} is needed for nucleation to take place.[147] Because the concentration of water vapor is much larger than that of sulfuric acid, it is assumed to remain unchanged by the hydration of the acid.

We have calculated the equilibrium sulfuric acid hydrate distribution at 20%, 50%, and 100% relative humidity (RH). As shown in the top right-hand side of Figure 11, at the top of the troposphere where the temperature is 217 K and the

dx.doi.org/10.1021/jp3054394 | J. Phys. Chem. A 2012, 116, 9745−9758

concentration of water vapor is 9.9×10^{14} cm^{-3} at 100% RH, the concentration of water drives the formation of the singly hydrated sulfuric acid up to four added water molecules. For a fifth water, the dimeric sulfuric acid cluster with $n = 5$ now exceeds the concentration of a monomeric sulfuric acid with $n = 5$, and both concentrations fall off to less than 1000 clusters/cm^3 when $n = 6$. At 20% relative humidity (top left-hand side of Figure 11), the concentrations of the monomeric sulfuric acid clusters fall off faster, and there are virtually no monomeric or dimeric clusters present with six water molecules. The bottom of Figure 11 shows that at room temperature the equilibrium thermodynamics combined with the initial concentrations of water and sulfuric acid lead to the complete production of monomeric sulfuric acid clusters, with virtually no $(H_2SO_4)_2(H_2O)_n$ clusters produced.

Figure 11 shows that the sulfuric acid monomer hydrates form in much larger quantities than the dimer hydrates. The ratio of the concentration of sulfuric acid dimer hydrates to monomer hydrates is about 10^{-3} at 216.65 K and 10^{-6} at 298.15 K, 100% RH in an equilibrium situation. The difference grows rapidly with increasing temperature but has a weak dependence on the relative humidity. Both the ratio of dimeric to monomeric hydrates and the small RH dependence of the dimeric hydrate concentration are in fairly good agreement with predictions by Hanson and Lovejoy.[148] From the different conditions they considered, the ratio of the dimeric to monomeric hydrates was largest ($\sim 10^{-2}$) at $[H_2SO_4] = 1.3 \times 10^9$ cm^{-3} and $T = 233$ K; at higher temperatures, the ratio was 10^{-3} or smaller. On the other hand, Petäjä et al.[149] observed sulfuric acid dimer to monomer ratios of about 0.1 even in ultraclean experimental conditions at 293 K and 22% RH. The presence of ternary species like ammonia and amines can possibly explain the discrepancy between the two works.[149−151]

Capillary liquid drop (CLD) model[35] and lab experiments[48] indicate that sulfuric acid is extensively hydrated even at low (<20%) relative humidity, yet our previous results on monomeric sulfuric acid predicted that 50−60% remains unhydrated at 20% RH and 298.15 K.[59] Because the ratio of dimeric to monomeric sulfuric acid hydrates is 10^{-3} or smaller under most conditions, the extent of hydration our calculations predict will remain small compared to CLD predictions and experiment. Because including the effect of hydration from a CLD model decreases nucleation rates by a factor of 10^3−10^8,[41] one reason for discrepancy between classical nucleation theory predictions and experimental observations could be an overestimation of sulfuric acid hydration in other models.[49] Our model predicts much less hydration than CLD, and the difference is a result of our $\Delta G(T)$ values of hydration, which are higher than classical estimates. Xu and Zhang[152] suggest that caution must be taken in estimating equilibrium hydrate distributions using calculated Gibbs free energies and concentrations of monomer vapors because equilibrium for the various nucleating species is rarely established due to low concentrations. They also argue that making the ideal gas assumption overestimates the translational entropy and gives Gibbs free energies that are too high. As a result, free energies computed using quantum mechanical methods in combination with the ideal gas, rigid rotor, and harmonic oscillator models do not exhibit nucleation barriers that are central to classical nucleation theory.

4.6. Atmospheric Implications. One of the ongoing debates in aerosol science is the relative importance of binary, ternary, and ion-induced nucleation in aerosol formation.[15] Sipilä et al. have suggested that H_2SO_4−H_2O binary nucleation can explain observed new particle formation rates at ambient concentrations of H_2SO_4 ($\sim 10^5$−10^7/cm^3) as long as the experimental techniques used can accurately measure the gaseous H_2SO_4 and efficiently detect small (<1.5 nm in diameter) particles.[24] By looking at the dependence of the nucleation rate on the concentration of the H_2SO_4 precursor, the authors concluded that the critical nuclei of this binary system must have one or two H_2SO_4 molecules. Recent studies have determined that the presence of other species like ammonia and amines in trace amounts explains the low dependence of the nucleation rate on the concentration of H_2SO_4.[29] Thus, binary nucleation by itself is not sufficient to achieve observed new particle formation rates under ambient conditions. Our thermodynamic results combined with mass balance effects provide a theoretical framework for why binary nucleation is not favorable. Ternary nucleation involving ammonia at atmospherically relevant concentrations enhances the nucleation rates, but by how much is still being debated. Galactic cosmic rays have been implicated as a possible source of ions, which increase new particle formation rates.

On the basis of the fundamental nucleation theorem, the power law dependence of the H_2SO_4−H_2O nucleation rate on H_2SO_4 concentration has been used to determine the number of H_2SO_4 molecules in the critical cluster. This number varies with $[H_2SO_4]$, RH, T, and type of nucleation mechanism and is generally around 2 in atmospheric observations, yet lab measurements and theory suggest it should be a larger number. Some literature values at various $[H_2SO_4]$, RH, and T include 1−2,[9,13,18,24,153] 3−5,[29,147,154−157] 7−13,[158] or many more sulfuric acids.[6] Nevertheless, our results on sulfuric acid monomer and dimer hydration demonstrate that the growth of single sulfuric acid hydrates through the stepwise addition of water is thermodynamically limited. The combination of sulfuric acid monomer hydrates to form dimer hydrates is thermodynamically favorable as shown in Figure 9, but it is limited by the low concentration of sulfuric acid and its hydrates relative to water vapor. In spite of that, Petäjä et al. find that the rate of formation of sulfuric acid dimer is 2−4 orders of magnitude larger than that of 1.5 nm particles, a typical size of a critical cluster. Therefore, they conclude that the formation of sulfuric acid dimers is not the rate limiting step in the nucleation of sulfuric acid aerosols.[149] This work of Petäjä et al. does not rule out the presence of trace amounts of ternary species for aerosol formation. The recent CLOUD experiment determined that the presence of ammonia ($[NH_3] \sim 10^9$ cm^{-3}) increased the particle formation rates by a factor of 100−1000.[29] Lee and co-workers' laboratory measurements of binary and ternary homogeneous nucleation under atmospherically relevant conditions ($[H_2SO_4] = 10^6$−10^7 cm^{-3}, $[NH_3] = 10^9$−10^{12} cm^{-3}, and $T = 288$ K) showed that ammonia increases aerosol nucleation linearly by up to a factor of 10. This enhancement factor increases with decreasing sulfuric acid concentration and relative humidity.[156] A similar study with trimethylamine (TMA) reveals that at low relative humidity, TMA enhanced nucleation up to an order of magnitude greater than ammonia.[150] A recent kinetic study of the nucleation of a multicomponent system with sulfuric acid, water, ammonia, and amines provided evidence that both ammonia and amines can participate in particle nucleation and growth.[151] The enhancement of new particle formation due to ammonia and amines is related to their basicity, indicating that acid−base reactions (also referred to as base-stabilization[29]) is an important

dx.doi.org/10.1021/jp3054394 | J. Phys. Chem. A 2012, 116, 9745−9758

mechanism in aerosol nucleation and growth.[151] The effect of organic acids on the initial formation of molecular complexes may be sizable, but their contribution to particle growth is negligible due to their hydrophobicity.[27,159]

Using our Boltzmann averaged Gibbs free energies for both the sulfuric acid monomer and dimer hydrates, Figure 11 shows that the sulfuric acid monomer hydrates are at least 2 orders of magnitude more abundant than the dimer hydrates. The difference grows rapidly with increasing temperature but has a weak dependence on the relative humidity. This result is not surprising because the concentration of sulfuric acid (5×10^7 cm^{-3}) is much smaller than that of water vapor (10^{15}–10^{18} cm^{-3}). Therefore, what limits the formation of dimer hydrates is the concentration of sulfuric acid, not water. As shown in Figure 9, the combination of sulfuric acid monomers and/or its hydrates to form dimers and bigger clusters is thermodynamically favorable, but it might be kinetically limited because the concentration of the sulfuric acid monomers and hydrates is much smaller than that of water monomers.[13] The ratio of the number concentration of sulfuric acid dimer hydrates to monomer hydrates is about 10^{-3} at 216.65 K and 10^{-6} at 298.15 K, 100% RH in an equilibrium situation.

5. CONCLUSIONS

We have studied the thermodynamics of sulfuric acid dimer hydration using high-level ab initio calculations and explored its implication on acid dissociation and atmospheric aerosol formation. For $(H_2SO_4)_2(H_2O)_n$ where n = 0–6, we located the putative global and many low-lying local minima for each cluster size. The results provide a picture of the first deprotonation of sulfuric acid dimer hydrates to form di-ionic $[H_2SO_4(HSO_4^-)(H_3O^+)(H_2O)_{n-1}]$ and tetra-ionic $[(HSO_4^-)_2(H_3O^+)_2(H_2O)_{n-2}]$ clusters as a function of temperature for a system consisting of two sulfuric acid molecules and up to six waters. At 0 K, a sulfuric acid dimer undergoes the first acid dissociation of one sulfuric acid after the addition of only two waters and both acids after the addition of four waters. At 298.15 K, a sulfuric acid dimer undergoes the first acid dissociation of one sulfuric acid after the addition of three waters and both acids after the addition of five waters. As the sulfuric acids dissociate in the presence of waters, they form symmetric, charge separated structures that are energetically favorable but entropically constrained. The thermodynamics of sulfuric acid dimer hydration is favorable up to n = 5 at 298 K and n = 6 at lower temperatures. A much more thermodynamically favorable pathway for the formation of sulfuric acid dimer hydrates is through the combination of sulfuric acid monomer hydrates, but kinetic effects appear to limit that process due to the low concentration of sulfuric acid relative to water vapor at ambient conditions. The finding that two sulfuric acids begin to dissociate in the presence of fewer waters than does a single sulfuric acid may have important implications for solutions of concentrated sulfuric acid; we tentatively predict that the more sulfuric acid present the less water is necessary for acid dissociation to begin.

■ ASSOCIATED CONTENT

Supporting Information

Comparison of $H_2SO_4(H_2O)_n$ and $(H_2SO_4)_2(H_2O)_n$ thermodynamics, all the MP2/6-31+G* optimized Cartesian coordinates, VPT2/MP2/6-31+G* anharmonic frequencies, and RI-MP2/aVDZ electric dipole moments. This information is available free of charge via the Internet at http://pubs.acs.org/.

■ AUTHOR INFORMATION

Corresponding Author

*E-mail: george.shields@bucknell.edu.

Notes

The authors declare no competing financial interest.

■ ACKNOWLEDGMENTS

The authors thank Prof. Kari Laasonen of Aalto University for sharing the starting coordinates. Acknowledgment is made to the NSF and Bucknell University for their support of this work. This project was supported in part by NSF grant CHE-0848827, and by NSF grants CHE-0116435, CHE-0521063, and CHE-0849677 as part of the MERCURY high-performance computer consortium (http://www.mercuryconsortium.org).

■ REFERENCES

(1) Vaida, V.; Kjaergaard, H.; Feierabend, K. *Int. Rev. Phys. Chem.* **2003**, *22*, 203–219.
(2) Leopold, K. R. *Annu. Rev. Phys. Chem.* **2011**, *62*, 327–349.
(3) Foster, P.; Ramaswamy, V. Changes in Atmospheric Constituents and Radiative Forcing. In *Climate Change 2007 The Scientific Basis*; Solomon, S., Qin, D., Manning, M., Chen, Z., Marquis, M., Averyt, K. B., Tignor, M., Miller, H. L., Eds.; Cambridge University Press: Cambridge, U.K., 2007; pp 131–217.
(4) Castleman, A. W. J. *Space Sci. Rev.* **1974**, *15*, 547–589.
(5) Kulmala, M.; Vehkamäki, H.; Petäjä, T.; Dal Maso, M.; Lauri, A.; Kerminen, V. M.; Birmili, W.; McMurry, P. H. *J. Aerosol Sci.* **2004**, *35*, 143–176.
(6) Seinfeld, J. H.; Pandis, S. N. *Atmospheric Chemistry and Physics: From Air Pollution to Climate Change*, 2nd ed.; John Wiley & Sons, Inc.: New York, 2006.
(7) Headrick, J. E.; Vaida, V. *Phys. Chem. Earth. Pt. C* **2001**, *26*, 479–486.
(8) Vaida, V.; Daniel, J. S.; Kjaergaard, H. G.; Goss, L. M.; Tuck, A. F. *Q. J. R. Meteorol. Soc.* **2001**, *127*, 1627–1643.
(9) Kulmala, M.; Lehtinen, K. E. J.; Laaksonen, A. *Atmos. Chem. Phys.* **2006**, *6*, 787–793.
(10) Kulmala, M.; Riipinen, I.; Sipilä, M.; Manninen, H. E.; Petäjä, T.; Junninen, H.; Maso, M. D.; Mordas, G.; Mirme, A.; Vana, M.; et al. *Science* **2007**, *318*, 89–92.
(11) Weber, R. J.; Marti, J. J.; McMurry, P. H.; Eisele, F. L.; Tanner, D. J.; Jefferson, A. *J. Geophys. Res.* **1997**, *102*, 4375–4385.
(12) Kulmala, M.; Vehkamki, H.; Petäja, T.; Dal Maso, M.; Lauri, A.; Kerminen, V. M.; Birmili, W.; McMurry, P. H. *J. Aerosol Sci.* **2004**, *35*, 143–176.
(13) Kuang, C.; McMurry, P. H.; McCormick, A. V.; Eisele, F. L. *J. Geophys. Res.* **2008**, *113*, D10209.
(14) Kulmala, M.; Kerminen, V.-M. *Atmos. Res.* **2008**, *90*, 132–150.
(15) Zhang, R.; Khalizov, A.; Wang, L.; Hu, M.; Xu, W. *Chem. Rev.* **2012**, *112*, 1957–2011.
(16) Zhang, R.; Suh, I.; Zhao, J.; Zhang, D.; Fortner, E. C.; Tie, X.; Molina, L. T.; Molina, M. J. *Science* **2004**, *304*, 1487–1490.
(17) Zhao, J.; Khalizov, A.; Zhang, R. Y.; McGraw, R. *J. Phys. Chem. A* **2009**, *113*, 680–689.
(18) Metzger, A.; Verheggen, B.; Dommen, J.; Duplissy, J.; Prevot, A. S. H.; Weingartner, E.; Riipinen, I.; Kulmala, M.; Spracklen, D. V.; Carslaw, K. S.; et al. *Proc. Natl. Acad. Sci.* **2010**, *107*, 6646–6651.
(19) Wang, L.; Khalizov, A. F.; Zheng, J.; Xu, W.; Ma, Y.; Lal, V.; Zhang, R. *Nat. Geosci* **2010**, *3*, 238–242.
(20) Yu, F.; Turco, R. P. *Geophys. Res. Lett.* **2000**, *27*, 883–886.
(21) Curtius, J.; Lovejoy, E. R.; Froyd, K. D. *Space Sci. Rev.* **2006**, *125*, 159–167.
(22) Kerminen, V. M.; Petäjä, T.; Manninen, H. E.; Paasonen, P.; Nieminen, T.; Sipilä, M.; Junninen, H.; Ehn, M.; Gagné, S.; Laakso, L.; et al. *Atmos. Chem. Phys. Discuss.* **2010**, *10*, 16497–16549.
(23) Bzdek, B. R.; Zordan, C. A.; Pennington, M. R.; Luther, G. W., III; Johnston, M. V. *Environ. Sci. Technol.* **2012**, *46*, 4365–4373.

(24) Sipilä, M.; Berndt, T.; Petäjä, T.; Brus, D.; Vanhanen, J.; Stratmann, F.; Patokoski, J.; Mauldin, R. L.; Hyvarinen, A. P.; Lihavainen, H.; et al. *Science* **2010**, *327*, 1243−1246.
(25) Jiang, J.; Zhao, J.; Chen, M.; Eisele, F. L.; Scheckman, J.; Williams, B. J.; Kuang, C.; McMurry, P. H. *Aerosol Sci. Technol.* **2011**, *45*, ii−v.
(26) Lee, S.-H.; Allen, H. C. *Anal. Chem.* **2012**, *84*, 1196−1201.
(27) Zhang, R. *Science* **2010**, *328*, 1366−1367.
(28) Bzdek, B. R.; Johnston, M. V. *Anal. Chem.* **2010**, *82*, 7871−7878.
(29) Kirkby, J.; Curtius, J.; Almeida, J.; Dunne, E.; Duplissy, J.; Ehrhart, S.; Franchin, A.; Gagne, S.; Ickes, L.; Kurten, A. *Nature* **2011**, *476*, 429−433.
(30) Doyle, G. J. *J. Chem. Phys.* **1961**, *35*, 795−799.
(31) Mirabel, P.; Katz, J. L. *J. Chem. Phys.* **1974**, *60*, 1138−1144.
(32) Heist, R. H.; Reiss, H. *J. Chem. Phys.* **1974**, *61*, 573−581.
(33) Shugard, W. J.; Heist, R. H.; Reiss, H. *J. Chem. Phys.* **1974**, *61*, 5298−5304.
(34) Marvin, D. C.; Shugard, W. J. *J. Chem. Phys.* **1977**, *67*, 5982−5982.
(35) Jaecker-Voirol, A.; Mirabel, P.; Reiss, H. *J. Chem. Phys.* **1987**, *87*, 4849−4852.
(36) Kulmala, M.; Laaksonen, A. *J. Chem. Phys.* **1990**, *93*, 696−701.
(37) Laaksonen, A.; Kulmala, M. *J. Aerosol Sci.* **1991**, *22*, 779−787.
(38) Wyslouzil, B. E.; Seinfeld, J. H.; Flagan, R. C.; Okuyama, K. *J. Chem. Phys.* **1991**, *94*, 6842−6850.
(39) Kusaka, I.; Wang, Z. G.; Seinfeld, J. H. *J. Chem. Phys.* **1998**, *108*, 6829−6848.
(40) Noppel, M. *J. Chem. Phys.* **1998**, *109*, 9052−9056.
(41) Noppel, M.; Vehkamäki, H.; Kulmala, M. *J. Chem. Phys.* **2002**, *116*, 218−228.
(42) Vehkamäki, H.; Kulmala, M.; Napari, I.; Lehtinen, K. E. J.; Timmreck, C.; Noppel, M.; Laaksonen, A. *J. Geophys. Res.-Atmos.* **2002**, *107*, 4622.
(43) Bein, K. J.; Wexler, A. S. *J. Chem. Phys.* **2007**, *127*, 124316.
(44) McGraw, R. *J. Chem. Phys.* **1995**, *102*, 2098−2108.
(45) Arstila, H. *J. Chem. Phys.* **1997**, *107*, 3196−3203.
(46) Sorokin, A.; Vancassel, X.; Mirabel, P. *J. Chem. Phys.* **2005**, *123*, 244508.
(47) Yu, F. Q. *J. Chem. Phys.* **2007**, *127*, 054301.
(48) Marti, J. J.; Jefferson, A.; Cai, X. P.; Richert, C.; McMurry, P. H.; Eisele, F. *J. Geophys. Res.* **1997**, *102*, 3725−3735.
(49) McGraw, R.; Weber, R. J. *Geophys. Res. Lett.* **1998**, *25*, 3143−3146.
(50) Hanson, D. R.; Eisele, F. *J. Phys. Chem. A* **2000**, *104*, 1715−1719.
(51) Arstila, H.; Laasonen, K.; Laaksonen, A. *J. Chem. Phys.* **1998**, *108*, 1031−1039.
(52) Bandy, A. R.; Ianni, J. C. *J. Phys. Chem. A* **1998**, *102*, 6533−6539.
(53) Re, S.; Osamura, Y.; Morokuma, K. *J. Phys. Chem. A* **1999**, *103*, 3535−3547.
(54) Ding, C. G.; Taskila, T.; Laasonen, K.; Laaksonen, A. *Chem. Phys.* **2003**, *287*, 7−19.
(55) Ding, C. G.; Laasonen, K. *Chem. Phys. Lett.* **2004**, *390*, 307−313.
(56) Kurtén, T.; Torpo, L.; Ding, C. G.; Vehkamäki, H.; Sundberg, M. R.; Laasonen, K.; Kulmala, M. *J. Geophys. Res.* **2007**, *112*, D04210.
(57) Kurtén, T.; Sundberg, M. R.; Vehkamäki, H.; Noppel, M.; Blomqvist, J.; Kulmala, M. *J. Phys. Chem. A* **2006**, *110*, 7178−7188.
(58) Kurtén, T.; Noppel, M.; Vehkamäki, H.; Salonen, M.; Kulmala, M. *Boreal Environ. Res.* **2007**, *12*, 431−453.
(59) Temelso, B.; Morrell, T. E.; Shields, R. M.; Allodi, M. A.; Wood, E. K.; Kirschner, K. N.; Castonguay, T. C.; Archer, K. A.; Shields, G. C. *J. Phys. Chem. A* **2012**, *116*, 2209−2224.
(60) Shields, G. C.; Moran, T. F. *Chem. Phys. Lett.* **1983**, *101*, 287−290.
(61) Shields, G. C.; Moran, T. F. *J. Phys. Chem.* **1985**, *89*, 4027−4031.
(62) Shields, G. C.; Moran, T. F. *Theor. Chim. Acta* **1986**, *69*, 147−159.
(63) Shields, G. C.; Wennberg, L.; Wilcox, J. B.; Moran, T. F. *Org. Mass Spectrom.* **1986**, *21*, 137−149.
(64) Shields, G. C.; Steiner, P. A.; Nelson, P. R.; Trauner, M. C.; Moran, T. F. *Org. Mass Spectrom.* **1987**, *22*, 64−69.
(65) Jurema, M. W.; Kirschner, K. N.; Shields, G. C. *J. Comput. Chem.* **1993**, *14*, 1326−1332.
(66) Pickard, F. C.; Dunn, M. E.; Shields, G. C. *J. Phys. Chem. A* **2005**, *109*, 4905−4910.
(67) Pickard, F. C.; Pokon, E. K.; Liptak, M. D.; Shields, G. C. *J. Chem. Phys.* **2005**, *122*, 024302.
(68) Morrell, T. E.; Shields, G. C. *J. Phys. Chem. A* **2010**, *114*, 4266−4271.
(69) Husar, D. E.; Temelso, B.; Ashworth, A. L.; Shields, G. C. *J. Phys. Chem. A* **2012**, *116*, 5151−5163.
(70) Jurema, M. W.; Shields, G. C. *J. Comput. Chem.* **1993**, *14*, 89−104.
(71) Kirschner, K. N.; Shields, G. C. *Int. J. Quantum Chem.* **1994**, 349−360.
(72) Lively, T. N.; Jurema, M. W.; Shields, G. C. *Int. J. Quantum Chem.* **1994**, 95−107.
(73) Kirschner, K. N.; Sherer, E. C.; Shields, G. C. *J. Phys. Chem.* **1996**, *100*, 3293−3298.
(74) Sherer, E. C.; Turner, G. M.; Lively, T. N.; Landry, D. W.; Shields, G. C. *J. Mol. Model.* **1996**, *2*, 62−69.
(75) Sherer, E. C.; Yang, G.; Turner, G. M.; Shields, G. C.; Landry, D. W. *J. Phys. Chem. A* **1997**, *101*, 8526−8529.
(76) Shields, G. C.; Laughton, C. A.; Orozco, M. *J. Am. Chem. Soc.* **1997**, *119*, 7463−7469.
(77) Shields, G. C.; Laughton, C. A.; Orozco, M. *J. Am. Chem. Soc.* **1998**, *120*, 5895−5904.
(78) Sherer, E. C.; Bono, S. J.; Shields, G. C. *J. Phys. Chem. B* **2001**, *105*, 8445−8451.
(79) Kirschner, K. N.; Lexa, K. W.; Salisburg, A. M.; Alser, K. A.; Joseph, L.; Andersen, T. T.; Bennett, J. A.; Jacobson, H. I.; Shields, G. C. *J. Am. Chem. Soc.* **2007**, *129*, 6263−6268.
(80) Lexa, K. W.; Alser, K. A.; Salisburg, A. M.; Ellens, D. J.; Hernandez, L.; Bono, S. J.; Michael, H. C.; Derby, J. R.; Skiba, J. G.; Feldgus, S.; et al. *Int. J. Quantum Chem.* **2007**, *107*, 3001−3012.
(81) Shields, G. C.; Kirschner, K. N. *Synth. React. Inorg. Met.-Org. Chem.* **2008**, *38*, 32−36.
(82) Salisburg, A. M.; Deline, A. L.; Lexa, K. W.; Shields, G. C.; Kirschner, K. N. *J. Comput. Chem.* **2009**, *30*, 910−921.
(83) Dunn, M. E.; Pokon, E. K.; Shields, G. C. *J. Am. Chem. Soc.* **2004**, *126*, 2647−2653.
(84) Dunn, M. E.; Pokon, E. K.; Shields, G. C. *Int. J. Quantum Chem.* **2004**, *100*, 1065−1070.
(85) Day, M. B.; Kirschner, K. N.; Shields, G. C. *Int. J. Quantum Chem.* **2005**, *102*, 565−572.
(86) Day, M. B.; Kirschner, K. N.; Shields, G. C. *J. Phys. Chem. A* **2005**, *109*, 6773−6778.
(87) Dunn, M. E.; Evans, T. M.; Kirschner, K. N.; Shields, G. C. *J. Phys. Chem. A* **2006**, *110*, 303−309.
(88) Shields, R. M.; Temelso, B.; Archer, K. A.; Morrell, T. E.; Shields, G. C. *J. Phys. Chem. A* **2010**, *114*, 11725−11737.
(89) Temelso, B.; Archer, K. A.; Shields, G. C. *J. Phys. Chem. A* **2011**, *115*, 12034−12046.
(90) Temelso, B.; Shields, G. C. *J. Chem. Theory Comput.* **2011**, *7*, 2804−2817.
(91) Pérez, C.; Muckle, M. T.; Zaleski, D. P.; Seifert, N. A.; Temelso, B.; Shields, G. C.; Kisiel, Z.; Pate, B. H. *Science* **2012**, *336*, 897−901.
(92) Allodi, M. A.; Dunn, M. E.; Livada, J.; Kirschner, K. N.; Shields, G. C. *J. Phys. Chem. A* **2006**, *110*, 13283−13289.
(93) Alongi, K. S.; Dibble, T. S.; Shields, G. C.; Kirschner, K. N. *J. Phys. Chem. A* **2006**, *110*, 3686−3691.
(94) Kirschner, K. N.; Hartt, G. M.; Evans, T. M.; Shields, G. C. *J. Chem. Phys.* **2007**, *126*, 154320.

(95) Allodi, M. A.; Kirschner, K. N.; Shields, G. C. *J. Phys. Chem. A* **2008**, *112*, 7064−7071.
(96) Dunn, M. E.; Shields, G. C.; Takahashi, K.; Skodje, R. T.; Vaida, V. *J. Phys. Chem. A* **2008**, *112*, 10226−10235.
(97) Hartt, G. M.; Shields, G. C.; Kirschner, K. N. *J. Phys. Chem. A* **2008**, *112*, 4490−4495.
(98) Ding, C. G.; Laasonen, K.; Laaksonen, A. *J. Phys. Chem. A* **2003**, *107*, 8648−8658.
(99) Frisch, M. J.; Trucks, G. W.; Schlegel, H. B.; Scuseria, G. E.; Robb, M. A.; Cheeseman, J. R.; Montgomery, J. A.; Vreven, T.; Kudin, K. N.; Burant, J. C.; et al. *GAUSSIAN 09*, Revision B.02; Gaussian, Inc.: Wellington, CT, 2009.
(100) Feyereisen, M.; Fitzgerald, G.; Komornicki, A. *Chem. Phys. Lett.* **1993**, *208*, 359−363.
(101) Bernholdt, D. E.; Harrison, R. J. *Chem. Phys. Lett.* **1996**, *250*, 477−484.
(102) Neese, F. ORCA 2.8.0 - An ab initio, DFT and semiempirical SCF-MO package. Bonn, Germany. 2011. See http://www.thch.uni-bonn.de/tc/orca/; 2.8.0 ed., 2011.
(103) Dunning, T. *J. Chem. Phys.* **1989**, *90*, 1007−1023.
(104) Kendall, R.; Dunning, T.; Harrison, R. *J. Chem. Phys.* **1992**, *96*, 6796−6806.
(105) Woon, D.; Dunning, T. *J. Chem. Phys.* **1993**, *98*, 1358−1371.
(106) Weigend, F.; Kohn, A.; Hattig, C. *J. Chem. Phys.* **2002**, *116*, 3175−3183.
(107) Klopper, W. *J. Chem. Phys.* **1995**, *102*, 6168−6179.
(108) Xantheas, S. S. *Philos. Mag. B* **1996**, *73*, 107−115.
(109) Xantheas, S. S. *J. Chem. Phys.* **1996**, *104*, 8821−8824.
(110) Barone, V. *J. Chem. Phys.* **2004**, *120*, 3059−3065.
(111) Kim, K.; Jordan, K. D.; Zwier, T. S. *J. Am. Chem. Soc.* **1994**, *116*, 11568−11569.
(112) Pedulla, J. M.; Vila, F.; Jordan, K. D. *J. Chem. Phys.* **1996**, *105*, 11091−11099.
(113) Pedulla, J. M.; Kim, K.; Jordan, K. D. *Chem. Phys. Lett.* **1998**, *291*, 78−84.
(114) Bates, D. M.; Tschumper, G. S. *J. Phys. Chem. A* **2009**, *113*, 3555−3559.
(115) Nauta, K.; Miller, R. E. *Science* **2000**, *287*, 293−295.
(116) Steinbach, C.; Andersson, P.; Melzer, M.; Kazimirski, J. K.; Buck, U.; Buch, V. *Phys. Chem. Chem. Phys.* **2004**, *6*, 3320−3324.
(117) Vaida, V.; Headrick, J. E. *J. Phys. Chem. A* **2000**, *104*, 5401−5412.
(118) Pettersen, E. F.; Goddard, T. D.; Huang, C. C.; Couch, G. S.; Greenblatt, D. M.; Meng, E. C.; Ferrin, T. E. *J. Comput. Chem.* **2004**, *25*, 1605−1612.
(119) Diri, K.; Myshakin, E. M.; Jordan, K. D. *J. Phys. Chem. A* **2005**, *109*, 4005−4009.
(120) Kjaergaard, H. G.; Garden, A. L.; Chaban, G. M.; Gerber, R. B.; Matthews, D. A.; Stanton, J. F. *J. Phys. Chem. A* **2008**, *112*, 4324−4335.
(121) Curtiss, L. A.; Frurip, D. J.; Blander, M. *J. Chem. Phys.* **1979**, *71*, 2703−2711.
(122) Scribano, Y.; Goldman, N.; Saykally, R. J.; Leforestier, C. *J. Phys. Chem. A* **2006**, *110*, 5411−5419.
(123) Givan, A.; A. Larsen, L.; Loewenschuss, A.; J. Nielsen, C. *J. Chem. Soc., Faraday Trans.* **1998**, *94*, 2277−2286.
(124) Givan, A.; Larsen, L. A.; Loewenschuss, A.; Nielsen, C. J. *J. Chem. Soc.-Faraday Trans.* **1998**, *94*, 827−835.
(125) Givan, A.; Larsen, L. A.; Loewenschuss, A.; Nielsen, C. J. *J. Mol. Struct.* **1999**, *509*, 35−47.
(126) Hintze, P. E.; Kjaergaard, H. G.; Vaida, V.; Burkholder, J. B. *J. Phys. Chem. A* **2003**, *107*, 1112−1118.
(127) Vaida, V.; Kjaergaard, H. G.; Hintze, P. E.; Donaldson, D. J. *Science* **2003**, *299*, 1566−1568.
(128) Hintze, P. E.; Feierabend, K. J.; Havey, D. K.; Vaida, V. *Spectrochim. Acta Part a-Mol. Biomol. Spectrosc.* **2005**, *61*, 559−566.
(129) Mills, M. J.; Toon, O. B.; Vaida, V.; Hintze, P. E.; Kjaergaard, H. G.; Schofield, D. P.; Robinson, T. W. *J. Geophys. Res.-Atmos.* **2005**, *110*, D08201.
(130) Gerber, R. B.; Ratner, M. A. *Chem. Phys. Lett.* **1979**, *68*, 195−198.
(131) Miller, Y.; Chaban, G. M.; Gerber, R. B. *J. Phys. Chem. A* **2005**, *109*, 6565−6574.
(132) Sedo, G.; Schultz, J.; Leopold, K. R. *J. Mol. Spectrosc.* **2008**, *251*, 4−8.
(133) Brauer, C. S.; Sedo, G.; Leopold, K. R. *Geophys. Res. Lett.* **2006**, *33*, L23805.
(134) Fiacco, D. L.; Hunt, S. W.; Leopold, K. R. *J. Am. Chem. Soc.* **2002**, *124*, 4504−4511.
(135) Zangi, R. *J. Chem. Phys.* **2012**, *136*, 184501−184511.
(136) Vaida, V. *J. Chem. Phys.* **2011**, *135*, 020901.
(137) Sugawara, S.; Yoshikawa, T.; Takayanagi, T.; Shiga, M.; Tachikawa, M. *J. Phys. Chem. A* **2011**, *115*, 11486−11494.
(138) Robertson, W. H.; Johnson, M. A. *Science* **2002**, *298*, 69.
(139) Gutberlet, A.; Schwaab, G.; Birer, Ö.; Masia, M.; Kaczmarek, A.; Forbert, H.; Havenith, M.; Marx, D. *Science* **2009**, *324*, 1545−1548.
(140) Forbert, H.; Masia, M.; Kaczmarek-Kedziera, A.; Nair, N. N.; Marx, D. *J. Am. Chem. Soc.* **2011**, *133*, 4062−4072.
(141) Bianco, R.; Hynes, J. *Theor. Chem. Acc.* **2004**, *111*, 182−187.
(142) Bianco, R.; Wang, S. Z.; Hynes, J. T. *J Phys Chem B* **2005**, *109*, 21313−21321.
(143) Ianni, J. C.; Bandy, A. R. *J. Mol. Struct.: THEOCHEM* **2000**, *497*, 19−37.
(144) Nadykto, A. B.; Yu, F. *Chem. Phys. Lett.* **2007**, *435*, 14−18.
(145) Torpo, L.; Kurtén, T.; Vehkamäki, H.; Laasonen, K.; Sundberg, M. R.; Kulmala, M. *J. Phys. Chem. A* **2007**, *111*, 10671−10674.
(146) Salonen, M.; Kurtén, T.; Vehkamäki, H.; Berndt, T.; Kulmala, M. *Atmos. Res.* **2009**, *91*, 47−52.
(147) Berndt, T.; Boge, O.; Stratmann, F.; Heintzenberg, J.; Kulmala, M. *Science* **2005**, *307*, 698−700.
(148) Hanson, D. R.; Lovejoy, E. *J. Phys. Chem. A* **2006**, *110*, 9525−9528.
(149) Petäjä, T.; Sipilä, M.; Paasonen, P.; Nieminen, T.; Kurtén, T.; Ortega, I. K.; Stratmann, F.; Vehkamäki, H.; Berndt, T.; Kulmala, M. *Phys. Rev. Lett.* **2011**, *106*, 228302.
(150) Erupe, M. E.; Viggiano, A. A.; Lee, S. H. *Atmos. Chem. Phys.* **2011**, *11*, 4767−4775.
(151) Yu, H.; McGraw, R.; Lee, S.-H. *Geophys. Res. Lett.* **2012**, *39*, L02807.
(152) Xu, W.; Zhang, R. *J. Phys. Chem. A* **2012**, *116*, 4539−4550.
(153) Hanson, D. R.; Eisele, F. L. *J. Geophys. Res.* **2002**, *107*, 4158.
(154) Eisele, F. L.; Hanson, D. R. *J. Phys. Chem. A* **2000**, *104*, 830−836.
(155) Nadykto, A. B.; Yu, F.; Herb, J. *Int. J. Mol. Sci.* **2008**, *9*, 2184−2193.
(156) Benson, D. R.; Yu, J. H.; Markovich, A.; Lee, S. H. *Atmos. Chem. Phys.* **2011**, *11*, 4755−4766.
(157) Zhao, J.; Eisele, F. L.; Titcombe, M.; Kuang, C.; McMurry, P. H. *J. Geophys. Res.* **2010**, *115*, D08205.
(158) Ball, S. M.; Hanson, D. R.; Eisele, F. L.; McMurry, P. H. *J. Geophys. Res.* **1999**, *104*, 23709−23718.
(159) Zhang, R.; Wang, L.; Khalizov, A. F.; Zhao, J.; Zheng, J.; McGraw, R. L.; Molina, L. T. *Proc. Natl. Acad. Sci.* **2009**, *106*, 17650−17654.